DRA

PLANETARY SCIENCE INSTITUTE

(NASA-CR-155310) LOW-SPEED IMPACT PHENOMENA AND ORBITAL RESONANCES IN THE MOON- AND PLANET-BUILDING PROCESS Semiannual Report (Planetary Science Inst., Tucson, Ariz.) 73 p HC A04/MF A01 CSCL 03B G3/90

N78-19016

Unclas 15120

MAR 1978
RECEIVED
NASA STI FACILITY

JAN 1978
RECEIVED
NASA STI FACILITY

SEMI-ANNUAL REPORT

LOW-SPEED IMPACT PHENOMENA AND ORBITAL RESONANCES IN THE MOON- AND PLANET-BUILDING PROCESS

NASW-2909 (Mod 1)

December 30, 1977

Planetary Science Institute
2030 East Speedway, Suite 201
Tucson, Arizona 85719

SEMI-ANNUAL REPORT

LOW-SPEED IMPACT PHENOMENA AND ORBITAL RESONANCES IN THE MOON- AND PLANET-BUILDING PROCESS

Principal Investigator: Clark R. Chapman

The following manuscript constitutes our Semi-Annual Report on Contract NASW-2909 (Mod 1). It describes the work done and the progress made through November 21, 1977.

PLANETESIMALS TO PLANETS:
NUMERICAL SIMULATION OF COLLISIONAL EVOLUTION

by

Richard Greenberg

John F. Wacker*

William K. Hartmann

Clark R. Chapman

Planetary Science Institute

2030 East Speedway, Suite 201

Tucson, Arizona 85719

*Also, Department of Planetary Sciences, University of Arizona, Tucson, Arizona 85721.

ABSTRACT

A simulation of collisional and gravitational interaction in the early solar system generates planets $\sim$1000 km in diameter from an initial swarm of kilometer-sized planetesimals, such as might have resulted from gravitational instabilities in the solar nebula. The model treats collisions according to experimental and theoretical impact results (such as rebound, cratering, and catastrophic fragmentation) for a variety of materials whose parameters span plausible values for early solid objects. Ad hoc sticking mechanisms are avoided. The small planets form in $\sim 10^4$ yr, during which time most of the mass of the system continues to reside in particles near the original size. The relative random velocities remain of the order of a kilometer-sized body's escape velocity, with random velocities of the largest objects somewhat depressed due to damping by the bulk of the material. The simulation is terminated when the largest objects' random motion is of smaller dimension than their collision cross-sections, so that the "particle-in-a-box" statistical methods of the model break down. The few 1000 km planets, in a swarm still dominated by kilometer-scale planetesimals, may act as "seeds" for the subsequent, gradual, accretional growth into full-sized planets.

I. BACKGROUND

Currently fashionable models for the formation of the planets require collisional accretion of planetesimals. Earlier theories had suggested that planet-sized objects might have formed as a result of turbulent vorticity which concentrated solid material at certain locations in the solar nebula (cf. Kuiper, 1951a) or as a consequence of gravitational instabilities which would accompany the flattening of solid material into a disk (Kuiper, 1951b). More recently, Goldreich and Ward (1973) have shown that such effects might have produced planetesimals only a few kilometers in size in the region of the solar system now occupied by the terrestrial planets.

How, then, were planet-sized bodies built from these planetesimals? Safronov (1972) suggested that mutual collisions and accretion produced larger bodies which then swept up the smaller ones within their gravitational cross-sections and scattered other planetesimals onto orbits which permitted later accretion. Safronov's analytic approach required a decoupling of the evolution of random relative velocities of particles (i.e. orbital eccentricities and inclination) from the evolution of their size distribution. Safronov obtained the result that, once equilibrium is reached, relative velocities are comparable to the escape velocity

associated with that size particle which dominates the population, specifically the largest bodies in a reasonable power-law distribution. Many investigators have assumed that this condition applied throughout the growth process. Under this assumption Safronov modelled the evolution of the size distribution which yielded planet-sized objects whose final stages of accretion involved high velocity collisions which produced such observed properties as the distribution of obliquities and rotation rates of planets.

This picture of planet growth has been refined by considering possible high velocity components of the colliding population. Weidenschilling (1974) hypothesized that Jupiter grew earlier than the terrestrial planets because low temperature would have led to early condensation of more, and possibly stickier, solid matter. He suggested that Jupiter may have played a role in promoting accretion of terrestrial planets by inducing relative velocities among planetesimals, thus increasing the accretionary flux on the growing bodies. Weidenschilling (1975) and Kaula and Bigeleisen (1975) have proposed models in which planetesimals scattered by close encounters with Jupiter have different effects on each of the early terrestrial bodies and account for important differences in observed physical properties.

Another source of enhanced relative velocities would have been resonances between the orbits of planetesimals and Jupiter. The possible importance of such resonances was stressed by Safronov (1972, p. 89) and by Kuiper (1974).

However, a meaningful model of planet growth near resonance cannot be constructed by simply increasing relative velocities in Safronov's analysis because the induced relative velocities are size dependent (Greenberg, 1978). In fact, if we are to incorporate such sophisticated, but essential, mechanisms as orbital resonances into our ideas about planet growth, we must first devise a model that includes the coupled evolution of the size and velocity distribution.

We have undertaken to develop such a comprehensive numerical model for the evolution of already-formed swarms of planetesimals into small planets. Our aim is to include a wider variety of physical processes (e.g. resonances) and more detailed treatment of certain ones (e.g. low-velocity impact phenomena) than has been attempted before. The model has been developed and extended from an earlier model of Chapman and Davis (1975) which was intended to treat high-velocity asteroid fragmentation processes. The new model has provision for treating the entire range of planetesimal velocities and for treating both erosion and accretion, in addition to the catastrophic fragmentation processes already part of the original model.

A fundamental element of this project is the careful evaluation -- both experimentally and theoretically -- of the nature of low- and moderate-velocity collisional interactions among solid bodies. This approach contrasts with previous models. For instance, the numerical simulation by Isaacman and Sagan (1977) ignores collisional mechanics

and simply assumes 100% efficient accretion of any particle impacting sequentially introduced accretion nucleii, with no possibility of other particles sticking together. Very few experiments have been conducted previously of fragmentation and cratering processes at velocities much less than the hypervelocities that exist in the solar system today. It is expensive and time-consuming to investigate the entire range of velocities, projectile/target diameters, material properties, etc. for the whole suite of relevant parameters (rebound velocities, fragmental and ejecta size and velocity distributions, etc.). But through judicious selection of several low-velocity experiments combined with interpolation based upon physical principles, we can gain a much better understanding of the low-velocity interaction of planetesimals.

II. THE ALGORITHM

In this paper, we report on the development of a computer simulation of the collisional evolution which includes the simultaneous variation of velocity- and mass-distributions with time. In this respect the model represents a significant advance toward an accurate portrayal of early events in the solar system. However, many important phenomena have yet to be included, and many parameters, such as the strength of the relevant material, can only be estimated. Nevertheless our algorithm provides a basis for a higher-order approximation of the evolution, and for study of the relative

influence of various phenomena and parameters.

The population of particles in the collisionally evolving swarm is represented by a size distribution N(D), the number of particles per log increment in diameter D and over a particular range of semi-major axes, a to a+Δa. This function is represented numerically by the numbers of objects in each of the increments of log D over the size range under study. Each of these "size bins" has a particular variable value of the eccentricity e and of the inclination i associated with typical particles of that size. Ideally, one would like to have a distribution of e's and i's associated with each size bin, but this would increase the number of dimensions to an unmanageable degree, although ultimately it may be possible to include at least some parameterization of distributions in e and i. The e's and i's provide a measure of the random relative velocities among particles and the i's determine the thickness of the disk of particles in each size bin. We consider the events in a series of short time steps. In each time step, the probable number of collisions between particles in each pair of size bins is computed by a simple "particle-in-a-box" estimate:

$$\text{Number of collisions} = \frac{N_1 N_2 \; v_{rel} \times (\text{cross section}) \times \Delta \text{ time}}{\text{volume of space}}$$

where N_1 and N_2 are the number of particles in two size bins, v_{rel} is the mean relative velocity computed from e's and i's

for both bins, the cross-section represents the geometrical cross-section enhanced by gravitational focusing, and the volume is determined from a, Δa, and the disk thickness. Given the masses and velocities involved in each collision we determine the outcome of the collision in terms of resulting size distribution of ejecta, debris, or fragments and resulting relative velocities. The population distribution is then adjusted according to the number and outcome of collisions of each of several types discussed below. The e's and i's are modified by averaging in the new relative velocities of those particles which come out of collisional events. Time steps are chosen so that all changes in size and velocity in any one step are small.

Collision Outcomes

In order to implement this program we require some model of the outcome of collisions as a function of mass ratio and relative velocity at impact. For rocky materials experimental data are sparse compared with the wide range of masses and velocities required in our model. For this reason our model inevitably involves considerable extrapolation, which must be reconsidered as more relevant data become available. For now our algorithm divides the results of impact into four general categories, discussed in turn below: (i) Elastic rebound, (ii) Rebound with cratering of both surfaces, (iii) Shattering of the smaller body and cratering of the larger one, (iv) Shattering of both bodies.

(i) Elastic rebound. Impact at sufficiently low velocity between cohesive elastic bodies will result in rebound without chipping or cratering of either surface. Upon impact the surface of each body is depressed at a velocity v about half the impact velocity. The stress is alleviated primarily by propagation of a compressional wave at sound velocity c so that the maximum strain is $\sim v/c$. The maximum stress using the elastic modulus $c^2\rho$ would be $c\rho v$ which must be less than the crushing strength S to prevent local fracture. For reasonable rock values this requires $v < 5$ m/sec or impact velocity < 10 m/sec. Indeed, our experiments show a transition between no observable chipping at less than 10 m/sec to significant chipping at greater than 20 m/sec.

The rebound velocity for basalt spheres at such low velocities is about 85% of impact velocity (Hartmann, 1978); for non-rotating irregular shaped rocks where substantial energy of collision goes into changing the rotation, this coefficient of restitution, c_i, is often less than 50% (Hartmann, 1978).

In our program the upper limit impact velocity for elastic rebound, v_c, and coefficient of restitution are variable impact parameters. If the impact velocity (the mean relative approach velocity augmented by the mutual gravitational acceleration) is less than the upper limit, the bodies separate at a velocity governed by the coefficient of restitution. If this separation velocity is less than the mutual escape velocity, the particles combine to produce a new particle whose mass is

the sum of their masses and with e and i dictated by the in-plane and out-of-plane components of the mean velocity of the center of mass of the two colliding particles with respect to circular orbits. If the rebound velocity is great enough to permit mutual escape, the particles remain distinct with their e's and i's changed to reflect the change in relative velocities.

For bodies with regolith surfaces or with an intrinsically weak nature, such as primitive carbonaceous chondritic material, the upper velocity limit, v_c, for regime (i) might be practically zero. This type of material might well be representative of early solar system rocky condensates so collisions in regime (i) might never have occurred. On the other hand the treatment of this regime is incorporated into the program to permit flexibility in the types of material which can be studied. Conceivably, depending on heating mechanisms, early material might have achieved characteristics of hard rock shortly after accretion. We know that rocky and metallic bodies exist today.

(ii) Rebound with cratering of both bodies. If the rebound limit of (i) is exceeded but neither body is catastrophically disrupted, the surfaces of the impacting bodies will be locally damaged, e.g. chipped or cratered. (Hereinafter we shall refer to all such local damage as "cratering".) We know of no experimental results which give data specifically for this regime. On the other hand, there exist experimental

results in which high-velocity projectiles deliver kinetic energy to the surfaces of semi-infinite targets, thus producing craters. The mass excavated by these events can be approximated as a constant, K, times the kinetic energy delivered. Marcus (1969) summarizes results of Gault which give this constant K as $\sim 8 \times 10^{-10}$ cgs for basalt, $\sim 1.5 \times 10^{-9}$ cgs for "weakly bonded quartz sand", and $\sim 2 \times 10^{-8}$ for sand. In our algorithm we assume that half the kinetic energy of impact is delivered to each body in the colliding pair and we input some value of K within the plausible range to evaluate the mass cratered from each.

The cratering process removes mass from each body, whereupon the bodies rebound at some fraction, c_{ii}, of their impact velocity. This modified coefficient of restitution is less than the coefficient used in case (i) due to the loss of energy in cratering and mass ejection at the impact site. Indeed, in our experiments we have observed cases where a basalt ball or irregular igneous rock is fired into a rock target at 19 to 26 m/sec and undergoes minor cratering with modified rebound; in the two measured cases with basalt balls, the cratered projectile rebounded from impacts at 26 and 29 m/sec with velocity 0.73 and 0.90 times the normal rebound velocity, respectively. For weak materials the modified coefficient of restitution might be as low as 0.001. Just as for case (i), the computer program checks whether the rebound velocity permits separation or accretion of these bodies.

What can we say about the velocities of the crater ejecta? The best available data on crater ejecta velocity was given by Gault, Shoemaker and Moore (1963). They provided a plot estimating the cumulative mass of ejecta vs. velocity for cratering into basalt at velocity $\sim$6 km/sec (Fig. 1, heavy line). This result must be extrapolated over a great range of velocities, materials, and mass ratios. Therefore, we have introduced a simplified version of their result (Fig. 1, dashed line). Features such as the high velocity ejecta jet have been neglected as being too detailed for our degree of extrapolation. Marcus (1969) applied the same simplified curve for basalt to impacts in sand or regolith. His estimate was unreasonable because combined with the large value of K for sand, it gave the ejecta more kinetic energy than was put into the system by the impact! In fact, Stöffler, et al. (1975) show that ejecta from craters in sand at 6 km/sec travels $\sim 10^{-4}$ times as far as for a comparable event in basalt. Hence we hypothesize that the velocities for sand can be represented by shifting the curve for basalt leftward by a factor of 10^{-2} as shown in Fig. 1. A major problem is applying these crater ejecta data to craters formed at lower velocities. The curve may be relatively independent of impact velocity if the percent of impact energy going into ejecta kinetic energy does not vary with velocity. Applying this argument, Gault et al. (1963) estimated that impacts into basalt at tens of km/sec would give curves close to their 6 km/sec result.

We have performed experiments at much lower impact velocities; 6 m/sec impacts in vacuum into fine rock powders give ejecta velocities consistent with the estimate for sand in Fig. 1.

For real early solar system materials the relevant curve for cumulative fraction (f) of ejecta with velocity greater than v may resemble the intermediate curve: $f \approx c_{ej} v^{-9/4}$ where $c_{ej} = 3 \times 10^6$ cgs. The coefficient c_{ej} is an input parameter for the algorithm. The fraction of ejecta escaping from the parent body is given by the value of f which corresponds to the parent's escape velocity. If that value of f is less than 1, the bulk of the escaping ejecta barely escapes so we take the e and i values to be the same as those of the parent body. Here by "parent body" we mean the body from which the pieces were ejected or, if they accrete one another, we mean the combined body. If the escaping fraction is unity, the ejection velocity before escape is taken to be the value at which the f vs. v function intercepts f = 1.

How are the ejecta distributed in size? Based on experiments, observations of natural fragments, and earlier literature, Hartmann (1969) found a size distribution $N \propto m^{-2/3}$ where N is the number of particles with mass greater than m. This -2/3 power law applies to cases in which the locally damaged region receives barely enough energy for breakage and ejection. The largest piece has a mass given by setting N = 1. The constant must have a value $(M/2)^{2/3}$, where M

is the total mass of escaped ejecta, in order to conserve mass. For cases in which an excessive energy density is applied to the damaged region, Hartmann found that the power law exponent is closer to -1. This result pertains for cases of impact velocity greater than the speed of sound in the material (i.e. "hypervelocity" impact), because energy propagates away from the impact site slowly compared to the rate of impact energy delivery.

(iii) Smaller body shattered and larger one cratered. If sufficient energy is imparted to an entire body, it will fragment catastrophically, rather than experience merely local cratering. What are the criteria for catastrophic fragmentation? Most collision experimentation has dealt with hypervelocity cratering in semi-infinite targets. In such cases, the target is damaged only locally while the "bullet" undergoes super-catastrophic failure. Only a few experiments have been performed with targets small enough to yield results near the catastrophic limit. Theoretical evaluation of impact strength (Harris, 1975) has been unsuccessful because the processes involved are so complex (superposition of surface-reflected seismic waves, energy loss to heat and rotation, etc.). We have performed experiments with both finite and semi-infinite targets at a range of velocities (3-300 m/sec). Catastrophic failure occurs if a critical energy per unit volume is delivered to a body by an impact. In most collision experiments there

is a sharp transition over a narrow range of energy densities from minute local cratering to massive body fracture. For rocky materials and water ice these values are estimated to be 3×10^7 and 2×10^5 ergs/cm^3, respectively (Hartmann, 1978; Greenberg et al., 1977). For dirt clods, which may have cohesive strength comparable to early solar system solids, Hartmann (1978) finds a value of $\sim 10^5$. This parameter ("impact strength") has the dimensions of strength (supportable force/area) but is conceptually distinct. Experiments by Moore and Gault (1965) and by Fujiwara et al. (1977) confirm the impact strength for basalt even at much higher impact velocities (1 - 3 km/sec). These results indicate that impact strength is independent of velocity.

Further experiments are needed to show how energy is partitioned between colliding objects, and whether impact strength depends on object size. In our model we assume tentatively that half the kinetic energy of impact is delivered into each body, and that strength is independent of size. Hence, with increasing energy of collision, the smaller body of a colliding pair will shatter before the larger one. Planetary cratering is generally in this category. Studies of such impact events usually emphasize the cratering process and ignore the fate of the shattered projectile. In our study, where collisions between bodies of comparable masses must be considered as well as between bodies of very different masses, we must consider the debris from the smaller body as well as the crater ejecta.

How are the pieces of the shattered body distributed? Hartmann (1969) noted that, just as crater ejecta, such debris follows a cumulative size distribution of the form $N = Cm^{-b}$ where C and b are constants; b varies from a value of about 2/3 for cases where fragmentation energy is minimal to about 1 where large amounts of excess energy are delivered. In order to construct a computer algorithm we needed to quantify Hartmann's observation. We may estimate the mass of the largest fragment by taking N = 1 which yields $m_{max} = C^{1/b}$. Integration gives the total mass of the fragments as $M = \left(\frac{bC}{1-b}\right) m_{max}^{1-b}$ where M equals the mass of the shattered body. We may solve for b and C in terms of m_{max} and find $b = \{(m_{max}/M) + 1\}^{-1}$ and $C = m_{max}^{b}$. All we need in order to determine the size distribution is a way to calculate m_{max}. Note that if m_{max} varies from M/2 (barely catastrophic) towards 0 (super-catastrophic), b varies from 2/3 to 1 in agreement with Hartmann's observation. Fujiwara et al. (1977) give $m_{max}/M = 2.82 \times 10^{8}$ (Energy/mass)$^{-1.24}$ for basalt; for other materials we scale the coefficient so that $m_{max} = M/2$ at the critical energy density.

The velocity of the fragments with respect to the impact site is computed such that all have the same speed and their kinetic energy is 50% of the energy delivered to the shattered body by the impact. This value is consistent with our experimental results for basalt and other igneous rocks at impact velocities of tens of meters per second, although we are neglecting any high velocity "tail" in the distribution. (In reality there must be some distribution of

debris velocities, but no relevant experimental data yet exist.) The algorithm checks whether the debris' velocity is sufficient to escape the larger body's gravitational field. If it is not, they fall back and accrete; otherwise, they escape and add to the numbers of smaller particles with their e's and i's averaged in with those of the pre-existing small particles.

(iv) Both bodies shattered. If the energy of collision is sufficiently great, both bodies will shatter. Again, we assume that half the energy goes into each body. The fragment size and velocity distribution for debris from each body is computed as for the smaller body in (iii). The total kinetic energy is compared with the gravitational binding energy. If sufficiently small, the debris fall back together; otherwise many small particles are created.

Fig. 2 summarizes our treatment of the collision outcomes as a function of mass ratio and impact velocity. Fig. 3 illustrates the change in particle mass for each outcome category.

Re-distribution of Sizes

The size distribution can be changed in two distinct ways in any time step. First, the number of particles in each size bin may be changed. For example, catastrophic fragmentation of a large body removes one body from its size bin and adds many bodies to smaller size bins according to the power law distribution. The second mode of re-distribution is

more subtle. Bodies in a given size bin may change mass, as in accretion or cratering erosion, by increments too small to effect a transfer into a new size bin. Such incremental changes are crucial to an evolution model, especially if accretional growth is expected. This requirement contrasts with the asteroid collision model of Chapman and Davis (1975) in which the dominant collisional process was assumed to be catastrophic fragmentation. In order to account for incremental changes in mass we adopt the following procedure. The number of particles in each size bin is assumed to be distributed uniformly in log D. During a time step the average change in mass is computed for particles in each bin. This shift in mass moves those particles at one end of the size bin into the next bin. The mass of particles shifted into the next bin is calculated and is used to compute a change in the number of particles in that next bin, in such a manner as to conserve mass. The e and i characteristic of the former bin are averaged into the e and i of the new bin.

Growth of the bodies in the largest size bin by accretion might shift some small portion of the bodies into a new largest size bin in each time step. In general, our algorithm suppresses this transfer until a sufficient mass change accumulates that the number of bodies transferred into the new bins is greater than one. Otherwise meaningless infinitesimal fractions of bodies would be placed into the large size bins.

Actually, the choice of unity for the lower limit on numbers in the new bin is arbitrary. A fractional number of particles in a size bin can have meaning since it is the number per size increment per semi-major axis increment. (Both of these increments are arbitrary with only the restrictions that size bins be sufficiently narrow that no important structure of the size distribution is neglected and that Δa be small enough that eccentricity and inclination give a good estimate of random velocities over the entire $\underline{a}$ range.) We have experimented with various values of the required number for opening a new largest bin and find that the characteristics of the evolution are relatively independent of this choice.

A different criterion for populating a new largest size bin is needed when the largest bodies are so large, and accrete so efficiently, that their masses increase very fast compared with their numbers. As they accrete one another according to the formalism of particle-in-a-box statistics, their numbers may decrease faster than smaller bodies grow to replenish their numbers. Hence, they may grow by an amount greater than the increment between size bins before the criterion described above permits a transfer of bodies into the next bin. For this reason we permit the transfer if the mass change is a significant fraction of the bin width, even if less than the normally required number is transferred into the new largest bin.

When the distribution reaches a stage where there are only a few bodies per A.U. over a significant range of the largest size bins, the system begins to be dominated by the statistics of small numbers which our program is not designed to treat. The final stages of planetary accretion are simply not amenable to the particle-in-a-box approach. However, as we shall show, our algorithm does work over an evolutionary period in which thousand-kilometer bodies are produced from a population originally all $\sim$1 km in diameter.

Re-distribution of Velocities

The orbital eccentricity and inclination represent the in-plane and out-of-plane components of the random relative velocity of particles with respect to purely circular Keplerian orbits. Collisions are assumed to result dominantly from these random motions, rather than from differential Keplerian velocities bringing bodies within their collisional cross-sections. For collisions between bodies from different size bins, the mean relative approach velocities are computed from both sets of random velocities. The mean in-plane and out-of-plane velocity components of the center-of-mass of the two colliding bodies are also computed. The collision outcome is then determined in the center-of-mass reference frame. Velocities of any debris, ejecta, or rebounding particles after escape are then added to the mean center-of-mass velocity. The mean in- and out-of-plane velocity components of escaping material are computed assuming isotropic escape with respect

to the center-of-mass of the colliding system. Any newly created particles are distributed into appropriate size bins and their velocities are root-mean-square averaged with the random velocities already associated with particles of their size, yielding a corresponding adjustment of e and i.

In general collisions tend to damp the random velocities, although this is not always the case. For example, a slow moving body may hit and rebound from a fast moving large one. Even if the coefficient of restitution is significantly less than one, the small body may gain kinetic energy. Safronov (1972) pointed out another mechanism that tends to increase random velocities: the gravitational interactions of close approaches. With a number of approximations and assumptions he performed an analysis which indicated that an equilibrium between this stirring effect and collisional damping would yield random velocities on the order of the escape velocity of the dominant size particle.

In our program we numerically compute the change in random velocities in each time step due to gravitational stirring. Just as for each size particle we consider the probability and consequences of collisions with each other size particle, so we also consider the gravitational stirring as it passes through the field of particles of each other size. The ultimate source of gravitational stirring is the relative velocity between particles due to their differential Keplerian periods (cf. Safronov, 1972). Gravitational interaction rotates the relative motion so that a non-circular orbit is generated.

This randomizing of Keplerian shear is modelled in the following way. If a mass m_1 moves past another mass m_2, its velocity changes due to the gravitational interaction by an amount δv perpendicular to the initial relative velocity, v. This change is given by

$$\delta v = \frac{m_2 v}{m_1 + m_2} \sin 2\chi \quad , \tag{1}$$

where

$$\sin \chi = \left(1 + \frac{P^2 v^4}{G^2 (m_1 + m_2)^2}\right)^{-\frac{1}{2}} \tag{2}$$

P is the "impact parameter" (cf., Ward 1976). If m_1 moves through a field of particles of mass m_2, the mean square change in velocity per unit time is given for the planar case by

$$\frac{dv^2}{dt} = \int (\delta v)^2 \, \sigma \, v \, dP \quad . \tag{3}$$

where σ is the number of particles of mass m_2 per area of the disk.

If the velocity, v, is due to Keplerian shear, $v = \frac{1}{2}nP$ where n is orbital mean motion. This substitution and integration from small to large P yields approximately

$$\frac{dv^2}{dt} = G^{4/3} n^{1/3} \, (m_1 + m_2)^{-2/3} \, m_2^2 \, \sigma \, \frac{16\pi}{9\sqrt{3}} \tag{4}$$

We may show that this stirring model is consistent with Safronov's result by considering a simplified case with

all particles of equal size (mass m and diameter D). From Ward (1976) we get for the time scale for velocity damping due to energy loss in collisions in our notation

$$\tau = \left(\frac{1}{v}\frac{dv}{dt}\right)^{-1} \sim \frac{4}{\pi n D^2 \beta \sigma} \tag{5}$$

where β is the fractional energy loss per collision. Thus

$$\left(\frac{dv}{dt}\right)_{\text{damping}} \sim -\frac{\pi}{4} \; nD^2 \beta \sigma v \tag{6}$$

From (4) for $m_1 = m_2$:

$$\left(\frac{dv}{dt}\right)_{\text{shear}} \sim \frac{G^{4/3} \; n^{1/3} \; m^{4/3} \; \sigma}{v} \tag{7}$$

In equilibrium (6) and (7) are balanced so

$$v^2 \sim \frac{G^{4/3} \; m^{4/3}}{n^{2/3} \; \beta \; D^2} \sim \frac{v_e^2 \rho^{1/3} G^{1/3}}{4 n^{2/3} \beta} \tag{8}$$

where $v_e \equiv \sqrt{4Gm/D}$ is the escape velocity and $\rho \equiv 6m/(\pi D^3)$ is the material density. Taking $\rho \sim 3$ gm/cm^3, $\beta \sim 0.8$ and $n \sim 2\pi$/yr we obtain $v \sim 7\, v_e$.

The dependence of equilibrium random velocity on $n^{-1/3}$ is worthy of note. Over the entire solar system the random velocity varies by less than an order of magnitude. But beyond the distance of Pluto the random velocities would have been significantly higher than the particles' escape velocities, a factor which may have inhibited accretion at

such great distances from the sun. Moreover, for material around other stars with different masses, Kepler's third law gives a different mean motion for a given distance. The relation between mean motion and random relative velocities would limit the region in which planets might form. If this region fails to overlap the region in which temperature and pressure permit condensation, planet formation may be prohibited!

The analytic approach to velocity determination requires such assumptions as a simplified and constant mass distribution and velocity equilibrium. Our numerical approach requires none of these assumptions. We simply compute the change in velocity and mass distribution during each time step. Besides collisions, which primarily damp relative random velocities, and randomization of Keplerian differential velocities, we also take into account the rotation of random velocities due to gravitational encounters which can convert in-plane and out-of-plane motion from one to the other, thus partitioning random velocities between eccentricity and inclination.

III. NUMERICAL EXPERIMENTS AND RESULTS

Since knowledge of the relevant initial conditions, as well as material properties, is minimal, we must regard our computer simulation as a means of testing for the range of planetesimal conditions which lead to planet building. Does collisional evolution lead inevitably to growth of large bodies, or are very special initial velocities, mass distributions, and materials required? We have begun to test for the

generality of planet growth by selecting some plausible starting parameters and in subsequent numerical experiments varying these parameters to the limit of their reasonable range. So far, indications are that ∿1000-km bodies grow from 1-km bodies for a wide range of parameters and initial conditions. And they grow fast, on time scales of a few tens of thousands of years or less. For evolution beyond this stage we find that the random motion is too small to justify the "particle-in-a-box" statistics. These and other results will be discussed after the details of the various numerical experiments are presented.

Experiment 1 (Figs. 4, 5 and 6): Nominal Parameters

We have begun our numerical experiments by considering evolution near semi-major axis $a = 4 \times 10^{13}$ cm (about 2.7 AU) over a range (Δa) of 8×10^{11} cm (0.05 AU). We take the interval between size bins to be a factor of two in diameter. Initially we assume all bodies to have diameter 1 km as suggested by Goldreich and Ward's (1973) gravitational instability calculations We take 10^{12} as the initial number of such bodies, because, for a material density of $\rho \sim 3$ gm/cm^3, this number gives a surface density of the particulate disk of about 8 gm/cm^2, the value used by Goldreich and Ward in their calculations (comparable to the surface density computed by "spreading out" the mass of the present terrestrial planets over their portion of the present solar system; see also Lecar and Franklin, 1973).

For initial random velocities we selected values a few times the escape velocity of the 1 km bodies. A choice in this range seems appropriate in light of our discussion of equilibrium random velocities. Gravitational stirring would prohibit much lower velocities because v would be raised to several times v_e on a time scale $\sim$1000 years according to eqn. (7). A much greater initial velocity than we selected might lead to shattering and comminution of debris rather than planetary growth. (This occurred quite dramatically when we performed one run with weak material in which the initial velocity was about 20 v_e.) If this occurred in nature, one of two outcomes might result: (a) The comminuted debris might be removed by solar wind pressure, inhibiting planet growth by lowering the available mass or (b), if the comminuted debris is not removed, the material would reaccumulate into $\sim$1 km sized bodies by the Goldreich-Ward process. Because we know that planets ultimately did grow from that stage, at some point the velocities must not have been too much greater than a few times v_e.

The initial eccentricity and inclination for the planetesimals were each taken to be 5×10^{-4} which corresponds to random velocities of about 700 cm/sec, about nine times the escape velocity. We found that the first stage in the evolution is predominantly characterized by damping of this velocity down to less than half the initial value even

before any accretional growth takes place. Planet growth occurs independent of the choice of any initial velocity between 4 and 9 v_e.

In the first numerical experiment parameters were selected to approximate a material somewhat more loosely bonded than basalt, but more cohesive than merely gravitationally bound sand. (Parameters used for all experiments are summarized in Table 1.) The choice of K and c_{ej} means that about 3% of the impact kinetic energy goes into ejecta kinetic energy. The selected impact strength, $S = 3 \times 10^7$ ergs/cm^3, is perhaps somewhat too high to be consistent with the idea of weak early solar system materials, but later tests showed it doesn't seem to affect the evolution in a crucial way. Moreover, weak, loosely-bonded surface material does not necessarily imply that S is proportionately low. Conceivably, the interior would be packed more densely giving substantially greater resistance to catastrophic fragmentation than the surface properties would indicate. Also, such intrinsically weak material might be ineffective at propagating seismic energy of impact through its volume, thus inhibiting disruption.

The resulting evolution of the size distribution is shown in Fig. 4. The size distribution is shown near each time step at which bodies are placed in a previously unoccupied size bin. At each time step we output a matrix of outcomes

of collisions between bodies in each pair of size bins. For experiment 1, the matrix remained nearly constant throughout the evolution and is schematically shown in Fig. 5. Evolution of the eccentricity (in-plane random velocity) distribution is plotted in Fig. 6. (The inclination distribution is generally quite similar, within a few percent.)

For the first 10900 yrs, this evolution consists of collisions between 1 km bodies which crater one another but rebound and escape from one another. A small amount of crater ejecta escapes in each interaction, creating a distribution of small particles which in turn crater and escape one another and the 1 km bodies. The erosion of mass shifts some 1 km bodies into the 500m size bin, and these in turn erode into smaller sizes. In this manner, all the smaller bins are populated albeit with only a small fraction of the total mass. About 0.1% of the total system mass is lost beyond the smallest size bin (30 m) and is ignored in our program. The eccentricity of 1 km bodies damps down to about 0.00023 ($\sim 4\ v_e$) before accretion begins. The eccentricities of the smaller bodies damp down much more slowly because the bulk of the mass is in bodies much larger than themselves so gravitational stirring is more effective relative to collisional damping. This result may seem counter-intuitive to people who think of small bodies as generally being more susceptible to drag due to their large area/mass ratio.

Once the relative velocities of the 1 km bodies become low enough, the bodies begin to accrete one another. The sub-km

bodies never slow down enough to be accreted by the 1 km bodies. In fact, some of them have their random velocities pumped up by gravitational interaction with larger bodies. Bodies in diameter range 2 to ∿100 km accrete everything smaller that hits them. Bodies greater than ∿100 km accrete any impacting bodies after shattering them. Their greater gravitational cross-section permits more efficient accretion and hence introduces the reverse curve slope to the size distribution. A 500 km body is produced about 10,000 yr after accretion begins. By this time the statistics of small numbers must be important so our particle-in-a-box algorithm becomes invalid.

The most striking feature of this evolution is that most of the mass of the entire system remains in 1 - 4 km size bodies even after 100 - 500 km size bodies are produced. (This fact is made evident by comparison with a line in Fig. 4 whose slope is such that 8 times as many particles are in each succeedingly smaller box. A line of such slope represents equal mass per size bin.) The random velocities of the larger objects are damped by the 1 km bodies which appear to them as a dense, viscous medium. The random velocities of all bodies are quite low, on the order of the 1 km bodies' escape velocity as we would expect, because these bodies dominate the population. We conclude that in about 20,000 yr, a disk of 1 km bodies evolves to include a small number (∿25 per A.U.) of 300 - 700 km bodies in their midst. Such a small number of large bodies might form the seeds for subsequent growth of a few planets.

Experiments 2 & 3 (Figs. 7 & 8): Suppressed Ejecta Velocities

In order to demonstrate the minimal role played by crater ejecta in the evolution, we show (Experiment 2) a run executed with a somewhat different algorithm for ejecta distribution which effectively prevents escape of ejecta from its parent body. All ejecta were assumed to depart the surface with a velocity of 0.005 times the impact velocity, intermediate between the hypervelocity results of Stöffler et al. (1975) and of Gault et al. (1963). This rule, in effect, prohibits any ejecta from escaping its parent body. The resulting evolution is shown in Fig. 7. The results are virtually unchanged from the previous case for sizes 1 km or greater. The need to follow evolution over a smaller number of size bins permitted simulation over a greater time range than in Experiment 1 for the same given computer time limit. This resulted in creation and growth of 1000 km sized bodies after 24,000 yr, although the small-number statistics after the creation of 500 km objects give us little confidence in the validity of subsequent evolution.

This evolution was also simulated with a somewhat narrower value for the size bin interval, a factor of $2^{2/3}$ instead of 2 (Experiment 3). Again, the results (Fig. 8) are practically unchanged from those of Experiment 2 (Fig. 7), indicating that the size bin interval of a factor of 2 is sufficiently fine to model evolution adequately.

Experiment 4 (Fig. 9): Large Initial Population

In order to explore the importance of our choice of surface density of material in the disk, we ran one simulation

with 100 times as many 1 km objects as in the first run. The characteristics of the evolution (Fig. 9) were virtually identical with previous runs with one striking exception: the time scale was contracted by a factor of ~ 100. Creation of small particles from crater ejecta began almost immediately. Velocities of 1 km size bodies damped to $\sim 4\ v_e$ in 109 yr, at which time accretion began. A 500 km body was produced at $t = 157$ yr and a 1000 km body at $t = 179$ yr. At each stage in the accretion, (i.e. whenever a particle was created in a new bin) the eccentricity and inclination distribution was similar to that of the previous runs.

Experiment 5 (Figs. 10, 11, and 12): Solid Rock

Our next experiment gives some indication of the importance of the assumed material properties. As an extreme case we assume the material to have impact properties of solid, cohesive, competent rock. (See Table 1). The coefficients of restitution c_i and c_{ii} were both taken as 0.86, Hartmann's (1977) value for smooth basalt balls. For initial conditions, the same number of 1 km bodies and e and i were used as before. The results are shown in Figs. 10, 11 and 12. Initially, the 1 km bodies rebound after impact with one another. No cratering occurs. Their random velocity damps down for 109,500 yr until $e \approx i \approx 1.4 \times 10^{-5}$, equivalent to random velocity of $\sim v_e/4$. At this point, the energy lost in a collision is sufficient to prevent escape after rebound,

so accretion occurs. (The newly formed body is assumed to acquire strength properties comparable to the original material before the next impact. Since this is probably unrealistic, this solid rock case is clearly an extreme.) In a matter of a few years, bodies as large as 64 km are formed. While bodies between 1 and 32 km continue to rebound and accrete gravitationally, impacts into 64 km bodies are accelerated to sufficiently high velocities that cratering occurs, producing ejecta. As before, the ejecta never constitutes an important fraction of the mass in the system. Ejecta velocities are so high that the particles subsequently rebound without accretion from any bodies smaller than 64 km. The 1 km and larger bodies continue to accrete one another. Once bodies greater than 64 km are formed, they accrete any smaller impacting objects after shattering them. Within a hundred years after first accretion, bodies hundreds of kilometers in diameter are produced.

One striking property of this evolution is the hump in the size distribution (Fig. 10) at about 200 km. This may be an artifact due to the fact that, for the low approach velocities developed in this evolution, the formal gravitational collisional cross-section of a body greater than about 300 km exceeds its gravitational sphere of influence. The two body equations of motion used to compute the gravitation cross-section are invalid outside the sphere of influence, where solar gravity dominates. To model this effect in our algorithm, the cross-section is cut-off at the sphere of influence. Hence,

there may be a discontinuity in the efficiency of collisions for bodies greater than $\sim$300 km which would act as a dam slowing further growth and creating the 200 km hump.

Actually, the very low eccentricities and inclinations can be shown to invalidate evolution for this solid rock model for any bodies greater than about 40 km. These e's and i's correspond to excursions in distance $\sim ea = 10^9$ cm from circular motion. The gravitational cross-sections for bodies larger than 40 km are greater than 10^9 cm. The particle-in-a-box formulation is not applicable once the effective size of the particle is greater than its distance of random motion.

Why are random motions damped so effectively in this solid rock case? We might expect just the opposite: that the higher coefficients of restitution would give less damping. Indeed the damping is very slow: More than 10^5 yr elapse before relative velocities decrease enough for accretion to begin. But precisely because of the high coefficient of restitution, accretion can only begin after the approach velocities are considerably smaller than the 1 km bodies' escape velocity. For this reason, the eccentricities and inclinations of the growing bodies are small.

Recognizing that the particle-in-a-box model breaks down in Experiment 5 after bodies greater than $\sim$40 km have been created, we can make reasonable estimates of their subsequent

evolution based on our experience with collisional modelling. As these ∿40 km objects are formed they find themselves effectively isolated in nearly circular orbits. They sweep up all material which passes within their capture cross-section (10^9 cm) due to Keplerian differential motion. Continued growth of smaller bodies left in neighboring zones continues to produce more of these 40 km objects. Eventually, there are enough of these larger bodies that they begin to gravitationally stir one another into more irregular orbits (higher e's and i's). Henceforth, the particle-in-a-box assumption becomes applicable again. So long as the random velocities do not get too much greater than the larger bodies' escape velocities, accretional growth will then proceed.

Experiment 6 (Figs. 13, 14 and 15): Weakly Bonded Regolith

An opposite extreme of material properties was introduced by considering parameters appropriate to bodies consisting of loosely bonded regolith (Table 1). Again, the population was considered to consist initially of km-sized objects. Because of the low value of ρ compared to previous experiments, the initial number of bodies was augmented by a factor of 4 to keep the surface mass density of the disk ∿10 gm/cm^2. The escape velocity of the particles is reduced with the density, so we selected lower initial values for e and i of 7×10^{-5}, which is about 3 v_e.

The subsequent evolution is portrayed in Figs. 13, 14 and 15. It is quite similar to the general properties of previous experiments. The growth of bodies hundreds of km

in diameter occurs in about 1000 yr. This rate is much faster than for rock (Experiment 5) or for our intermediate strength material (Experiment 1), presumably because of the increased number of initial bodies in this case. It is slower than the case with initially larger numbers of particles (Fig. 9). The evolution begins with the 1 km bodies colliding, cratering, and accreting onto one another. The cratering generates small bodies and accretion creates many 4 km bodies within 30 yr. Any body smaller than 4 km continues to crater and accrete any other body of its own size that it hits. If it hits a smaller body, it is cratered and loses some mass and the smaller body shatters and escapes. The dominant process is accretion. When two bodies of equal size greater than 4 km collide, they shatter but remain gravitationally bound as a single object. If a body larger than 4 km hits a smaller body, the smaller body is shattered and accreted while the larger one is cratered with some ejecta escaping. The total mass of particles smaller than 30 m, which our program neglects, is less than 0.1% of the total. The pattern of collision outcomes (Fig. 15) is quite different than for previous cases, but the size distribution evolution (Fig. 13) follows a similar pattern. Bodies of hundreds of kilometer diameter are formed while most of the mass of the system remains in 1 km objects. The random velocities for the largest bodies are less than for the smaller ones, but all are of the same order as the escape velocity corresponding to diameter 1 km.

IV. DISCUSSION

The results just described are for only a few cases from the range of possible initial conditions and model parameters that one might wish to study. Moreover we have not yet incorporated some physical processes that we expect will be important, at least for some cases. Yet the results demonstrate dramatically the efficacy of planetesimal accretion. In this section, we discuss the significant consequences of our results and some areas in which we are continuing the work.

While there have been uncertainties about many stages of solar system origin and planetary accretion, one of the most serious questions has concerned the intermediate phase of accretion, i.e., growth after the hypothetical formation of planetesimals from gravitational instability (Safronov 1972; Goldreich and Ward 1973) but before the late stages of accretion when the largest bodies have substantial gravitational cross-sections (cf. Hartmann and Davis 1975). It has not been clear how planetesimals could have efficiently accreted one another. Our modelling, based on detailed physical experiments involving low-velocity collisions among rocky bodies, demonstrates that accretion through this intermediate size-range is efficient and rapid. It is a natural result of low-velocity rebound phenomena discussed by Hartmann (1978).

Some additional physical processes that might be important in this intermediate stage have not yet been incorporated into our numerical simulation. For instance, resonant phenomena might accelerate or retard growth in certain zones. Another influence

of interest is gas-drag, which seems even more relevant given the short time scales (10^4 years) in which we are getting substantial growth with our present algorithm. Possibly the influence of gas-drag on accreted bodies would not differ greatly from the influence of the swarms of small planetesimals remaining at the end of our simulations, but we intend to model gas explicitly in the future. A potentially disrupting influence on accretion would be high-velocity bodies, perhaps scattered into the zone of interest by an early-formed Jupiter.

Later Stages of Planet Growth

It is interesting to speculate on how later stages of planetary accretion might proceed, given the size- and velocity-distributions at the end of our simulations. Note that despite the development of 500 to 1000 km diameter objects, the bulk of the mass in the system remains in the 1 to 2 km diameter bins. Derivation of a similar result has been attributed to Y. Nakagawa by Hayashi *et al*. (1977). This state is similar to distributions used implicitly by several workers (Hartmann and Davis, 1977; Hayashi *et al*., 1977; Weidenschilling, 1974) as starting conditions for modelling the final stages of planetary growth: a few seed planets with most of the mass in a cloud of much smaller particles. Alternatively, before seeing our results, one might have imagined the intermediate stages to have been characterized by

such rapid growth of the smaller bodies that the largest bodies grew in numbers fast compared to their growth in size. If that were the case, the bulk of the mass would have resided in the larger bodies and the later stages of planet growth would have involved their mutual accretion, rather than accretion of planetesimals by seed planets hundreds of km in diameter. (A size distribution with most of its mass in the larger bodies is observed today in the asteroid belt, but this is probably a product of comminution rather than accretional evolution.)

While it is plausible that the first-formed multi-hundred km bodies will act as seeds for subsequent growth of full-sized planets, our present model cannot follow the detailed processes of such continued collisional evolution. This is because the random motions of the largest formed bodies have become, at this stage, smaller in extent than the dimensions of their gravitationally enhanced collision cross-sections. Thus our basic particle-in-a-box model breaks down because these bodies do not sweep through a representative sample of the entire population at a speed governed by random velocities. Instead,

a large body is encountered by, and accretes, only those smaller objects remaining with orbital semi-major axes close enough to the large body's that differential Keplerian velocities bring them within the collision cross-section. As this zone is cleared by accretion, it is conceivable that the large body's cross-section would grow so as to dominate an increasingly large annulus of planetesimals.

Alternatively, the large body may become effectively collisionally isolated from the rest of the system due to its nearly circular orbit. Such isolation would be only temporary. Diffusion by interactions of small-scale planetesimals from adjacent zones might tend to feed material into the large body's accretion zone. If that mechanism is slow or ineffective, continued collisional evolution among planetesimals in other zones would grow other 500 km scale bodies by the same process which led to the isolated first generation of large bodies. Eventually, there would be enough of these large bodies that they would begin to perturb one another onto more eccentric orbits providing access to one another and to any remaining planetesimals. Since the relative velocities due to stirring would be of the order of the large bodies' escape velocity, collisions thus promoted would probably result in accretion (Hartmann 1978). The gravitational scattering of planetesimals from the region of the first-formed full-size planet would also tend to break any isolation of 500 km objects.

Influence of Orbital Resonances

In addition, orbital resonances with the first-formed planet would have acted to break any such isolation by preferentially enhancing the orbital eccentricity of the larger bodies at certain semi-major axes, as consideration of the nature of these resonances will show. An orbital resonance occurs when a particle's orbital period is near a small whole-number commensurability with the period of the perturbing planet. Repetitive mutual configurations induce a forced eccentricity in the particle's orbit, the magnitude of which increases with decreasing distance from the exact commensurability (cf. Greenberg 1977). Similar effects ("secular resonances") occur near commensurabilities of precession periods.

The theory of resonances is a well-studied area of celestial mechanics so that computation of forced eccentricity is a straightforward procedure. However, a significant forced eccentricity at a given semi-major axis does not in itself imply enhanced relative velocities, because close particles undergo coherent perturbations: the apsides corresponding to the forced eccentricities are aligned in such a way as to minimize collisions. Those particles in a very narrow band near the exact resonance have large enough forced eccentricity that their radial excursion reaches particles whose motion is not coherent with their own. The particles in this narrow band transfer random motion to other particles in the vicinity through collisions. Such collisions could rapidly deplete the population of resonant particles unless new material is fed into the

resonance zone. This material might be either the scattered products of the collisions or material which has undergone secular variation of semi-major axis by drag or radiation effects.

The coherence of forced radial oscillation also breaks down at the sudden phase transition across the semi-major axis which corresponds to an exact resonance (Greenberg 1978). But this effect, too, involves only those particles extremely close to the critical semi-major axis.

On the other hand, different sized particles in a population do not have coherent resonant oscillation because, while the larger bodies' orbits respond to resonances and achieve an appropriate forced eccentricity, smaller bodies' orbits are drastically, discontinuously, and frequently modified by collisions with and close approaches to bodies of comparable or greater size. Hence, the smaller bodies cannot respond to long-term resonant perturbations. In this way forced eccentricities introduce a relative velocity between particles in different size regimes.

The distinction between the response of small and large bodies to resonant perturbations can be compared to the response of a mass hanging from a spring to a small periodic force close to its natural frequency. The resonant amplitude can be achieved only if the driving force operates for many periods and not if the position and velocity of the mass are frequently and arbitrarily re-initialized. These cases would be analogous to behavior of the larger and smaller bodies, respectively. Note that the larger bodies have their radial

oscillations damped by drag due to collisions with the small ones. The result is a phase shift and amplitude limit, just as would occur if drag were introduced to the mass-on-a-spring analog. These ideas are explored in more detail by Greenberg (1978).

Resonances are thus seen to provide an important mechanism for breaking the isolation of larger bodies during the accretion process due to their nearly circular orbits. On the other hand, the high relative velocities might have led to catastrophic fragmentation rather than accretion at these positions. Perhaps growth was favored just adjacent to the resonance positions where collisions were reasonably frequent but velocities were not too high.

Several properties of the present planetary distribution suggest that an accretional model governed by resonances may be relevant. The asteroid belt spans orbital radii which correspond to the important low-order commensurabilities with Jupiter's orbital period; planetesimals in the belt never grew to diameters much greater than 1000 km. [Chapman and Davis (1975) argue that, had they ever exceeded 1000 km, they would still survive.] The density distribution within the belt appears to be governed by resonances, with either gaps or concentrations at commensurable distances. In the outer solar system there are striking near-commensurabilities between adjacent planets (Wilkins and Sinclair 1974); satellite systems contain a statistically significant excess of resonances

(Goldreich 1965); and the structure of Saturn's rings appears governed by resonances with other satellites (Franklin and Colombo 1970). The terrestrial planets do not exhibit such striking mutual commensurabilities, but this might be explained by the shift in resonance positions which would have occurred in the presence of the early inner disk of material (more dense than in the outer solar system), just as resonances may be shifted in Saturn's rings according to the theory of Franklin and Colombo (1970).

Earliest Growth

Although we have applied our model to the intermediate stage of planet growth, it may also be relevant for earlier stages. In one test case, we applied our model to a case of mutual interaction in a population initially of all 1 cm particles. Bodies approaching 30 meters in diameter formed in only a few years. As in most of our other numerical experiments, most of the mass of the system remained in the initial-size particles at the time our particle-in-a-box approach became invalid, so it remains to be seen whether direct particle collisional interaction might be competitive in timescale with gravitational instability mechanisms for forming km-scale planetesimals.

Astrophysical Applications

Many astrophysicists have supposed that planet formation is a common process in the universe given the dusty clouds observed around newly formed stars. Yet so long as there

have remained obstacles to modelling the accretion of dust into full-sized planets, there has remained the possibility that the sun's planetary system is the result of unusual circumstances and that other planetary systems are rare. Thus our success in attaining rapid accretion through the difficult intermediate size ranges increases somewhat our expectation that planetary systems formed around some other stars.

While the numerical results reported here have concentrated on plausible early solar system models, we are currently broadening the range of input parameters to discover what conditions limit planet growth in the general stellar case. For example, one set of numerical experiments demonstrates conceptually how a sufficiently high velocity regime may completely inhibit growth of a planetary system and produce only a swarm of asteroid-like bodies. The experiments indicate that rock fragmentation will produce debris extending in size down to the size of the homogeneous grains in the shattered material. Our work suggests that the collisional evolution of planetesimals might produce abundant μm-scale particles which could be driven into interstellar space by radiation pressure (Soter, Burns, and Lamy, 1976). Thus planetesimal systems would be sources of observed interstellar grains as earlier suggested by Herbig (1970) and Hartmann (1970). Further details of this work will be reported in a future publication in preparation.

V. CONCLUSION

Our simulation is still undoubtedly a long way from complete reproduction of the collisional evolution of the early solar system. The list of physical mechanisms not incorporated in the model is presumably endless, although we must assume that most would have negligible effect on the results. Our algorithm may serve as the basis for testing the degree of importance of various phenomena. Certainly, the effects of gas drag, orbital resonances, and material scattered by Jupiter must be considered. As discussed in the introduction, our coupled treatment of evolution of mass and velocity distributions was largely motivated by the need to incorporate these phenomena. Our program is thus structured to permit such incorporation. The program is also designed to permit updating and refinement of the treatment of impact phenomena as more theoretical and experimental work is done. Inclusion of some other potentially important properties of the population may require structural modification to the algorithm. For example, surface regoliths and body rotation rates would evolve synergistically with size and velocity distribution during the collisional phase of planet formation (cf. Hartmann, 1978, regarding the relation with regoliths; Harris, 1977, regarding rotation), and these processes will be incorporated in our program in the future.

Besides providing a basis for future investigation of the relative importance of various phenomena, the simulation

is already a higher order approximation of collisional evolution than any constructed before. The main conclusions concerning growth of planets are the following: (a) Collisions beginning with km sized bodies rapidly produce a substantial number of 500 to 1000 km bodies. This result is based on an experimentally motivated model of impact outcomes. It requires no ad hoc sticking mechanism. (b) The bulk of the mass remains as km sized bodies even when the larger objects are formed. (c) Random velocities are of the order of the escape velocity of the original bodies, not of the large bodies. This result contrasts strikingly with the often-quoted conclusion of Safronov that velocities were on the order of the largest bodies' escape velocities. Safronov's result depended on the assumption of (i) a power-law size distribution with most mass in larger bodies and (ii) an equilibrium velocity solution. Our model is independent of such assumptions. In fact, neither assumption is justified since we show that most of the mass remains in small bodies and the growth of large ones occurs too quickly for equilibrium to be achieved. (d) Random motion is less for big bodies than small ones, because the big bodies experience drag due to the smaller ones, while the small ones are stirred by gravitational and collisional interactions with one another. (e) The creation of a small

number of bodies in excess of 500 km in a swarm still dominated in numbers and mass by much smaller objects suggests a picture of subsequent evolution in which the large bodies form seeds for the final stages of accretional growth. Further modelling which properly follows the statistical behavior of this small number of large bodies in terms of accretion and mutual interaction is needed to continue the study of collisional evolution through the formation of full-sized planets.

ACKNOWLEDGMENTS

This work was supported by NASA Grant NSG 7201 and by NASA Contract NASW-2909 with the Planetary Science Institute. Conversations with Dr. Donald R. Davis helped develop several important ideas. Computation was performed with the University of Arizona's CDC-6400 computer. This is P.S.I. Contribution Number 83.

REFERENCES

Chapman, C.R. and Davis, D.R. (1975). Asteroid collisional evolution: evidence for a much larger earlier population. Science 190, 553-556.

Franklin, F. and Colombo, G. (1970). A dynamical model for the radial structure of Saturn's rings. Icarus 12, 338-347.

Fujiwara, A., Kamimoto, G. and Tsukamoto, A. (1977). Destruction of basaltic bodies by high velocity impact. Icarus 31, 277-288.

Gault, D.E., Shoemaker, E.M. and Moore, H.J. (1963). Spray ejected from the lunar surface by meteoroid impact. NASA Tech. Note D-1767.

Goldreich, P. (1965). An explanation of the frequent occurrence of commensurable mean motions in the solar system. Mon. Not. Roy. Astron. Soc. 130, 159-181.

Goldreich, P. and Ward, W.R. (1973). The formation of planetesimals. Astrophys. J. 183, 1051-1061.

Greenberg, R. (1977). Orbit-orbit resonances in the solar system: varieties and similarities. Vistas in Astronomy 21, 209-239.

Greenberg, R. (1978). Orbital resonance in a dissipative medium. Icarus, in press.

Greenberg, R., Davis, D.R., Hartmann, W.K. and Chapman, C.R. (1977). Size distribution of particles in a planetary ring. Icarus 30, 769-779.

Harris, A.W. (1975). Collisional breakup in a planetary ring. Icarus 24, 190-192.

Hartmann, W.K. (1969). Terrestrial, lunar and interplanetary rock fragmentation. Icarus 10, 201-213.

Hartmann, W.K. (1970). Growth of planetesimals in nebulae surrounding young stars. In Evolution Stellaire avant la Sequence Principale 59, pp. 215-227, Univ. Liege Colloq.

Hartmann, W.K. (1978). Planet formation: mechanism of early growth. Icarus, in press.

Hartmann, W.K. and Davis, D.R. (1975). Satellite-sized planetesimals and lunar origin. Icarus 24, 505-515.

Hayashi, C., Nakazawa, K. and Adachi, I. (1977). Long term behaviors of planetesimals and the formation of the planets. Kyoto Univ. preprint KUNS 379.

Herbig, G.H. (1970). Introductory remarks. In Evolution Stellaire avant la Sequence Principale 59, pp. 13-26, Univ. Liege Colloq.

Isaacman, R, and Sagan, C. (1977). Computer simulations of planetary accretion dynamics: sensitivity to initial conditions. Icarus 31, 510-533.

Kaula, W.M. and Bigeleisen, P.E. (1975). Early scattering by Jupiter and its collision effects in the terrestrial zone. Icarus 25, 18-33.

Kuiper, G.P. (1951a). On the origin of the solar system. In Astrophysics (J.A. Hynek, ed), Chapter 8, McGraw-Hill, New York.

Kuiper, G.P. (1951b). On the origin of the solar system. Proc. Nat. Acad. Sci. 37, 1.

Kuiper, G.P. (1974). On the origin of the solar system. Celestial Mechanics 9, 321-348.

Lecar, M. and Franklin, F.A. (1973). On the original distribution of the asteroids. Icarus 20, 422-436.

Marcus, A.J. (1969). Speculations on mass loss by meteoroid impact and formation of planets. Icarus 11, 76-87.

Moore, H.J. and Gault, D.E. (1965). Fragmentation of spheres by projectile impact. Astrogeologic Studies, U.S.G.S. Annual Progress Report, 127-150.

Safronov, V.S. (1972). Evolution of protoplanetary clouds and formation of the earth and planets. NASA TT F-677.

Soter, S., Burns, J.A. and Lamy, P.L. (1976). Radiation pressure and Poynting-Robertson drag for small spherical particles. Proc. Internatl. Astr. Union Colloq. 39.

Stöffler, D., Gault, D.E., Wedekind, J. and Polkowski, G. (1975). Experimental hypervelocity impact into quartz sand: distribution and shock metamorphism of ejecta. JGR 80, 4062-4077.

Ward, W.R. (1976). The formation of the solar system. In Frontiers of Astrophysics, (E.H. Avrett, Ed.), Harvard Univ. Press, pp. 1-39.

Weidenschilling, S.J. (1974). A model for accretion of the terrestrial planets. Icarus 22, 426-435.

Weidenschilling, S.J. (1975). Mass loss from the region of Mars and the asteroid belt. Icarus 26, 361-366.

Wilkins, G.A. and Sinclair, A.T. (1974). The dynamics of the planets and their satellites. Proc. R. Soc. London A. 336, 85-104.

TABLE 1:

PARAMETERS FOR VARIOUS EXPERIMENTS.

ALL UNITS ARE CGS.

Experiment	#1, 2, 3, and 4	#5	#6
Comments:	Intermediate Material	Solid Rock	Loosely Bonded Regolith
Max. Vel. for Rebound w/o Cratering v_c	100	4000	1
Coeff. of Restitution c_i	0.5	0.86	0.01
Modified Coeff. of Rest. c_{ii}	0.1	0.86	0.001
Mass Excavated Coeff. K	10^{-8}	10^{-9}	3×10^{-7}
Ejecta Vel. Coeff. C_{ej} (cf. Fig. 1)	3×10^{6}*	2×10^{8}	10^{4}
Density ρ	3	4	0.9
Impact Strength S	3×10^{7}	3×10^{7}	10^{4}

*NOTE: In #2 and #3 all crater ejecta was given a velocity of 0.005 times impact velocity.

FIGURE CAPTIONS

Figure 1: The ejecta velocity distribution of Gault et al. (1963) for basalt (heavy curve) is approximated by a straight (dashed) line. Results of Stöffler et al. (1971) suggest velocities are a factor of 100 smaller for sand. The dotted segment is our extrapolation of the sand line beyond the range measured by Stöffler et al. We consider an intermediate distribution, with coefficient $c_{ej} = 3 \times 10^6$ cgs, as well.

Figure 2: Mapping of outcomes as function of impact velocity and mass ratio. Velocity V_c is upper limit for rebound. Catastrophic fragmentation (shattering) occurs if impact strength (critical energy/unit volume) is exceeded.

Figure 3: Schematic representation of our modeling of change in mass of an impacted body as a function of impact velocity and energy delivered to the body. Compare with Hartmann's experimental results (Hartmann, 1977, Figure 1).

Figure 4: Particle size distribution as a function of time for a material intermediate between loosely bonded regolith and solid rock, Experiment #1.

Figure 5: Matrix indicating results of collisions between pairs of bodies of various sizes in Experiment #1.

Code: 1 = Escape after outcome (i);

2 = Both bodies cratered (ii) and escaped from one another;

3 = One body shattered, its debris escapes other body;

4 = Both bodies shattered, debris escapes;

5 = Accretion after outcome (i) or (iv);

6 = Accretion after outcome (ii);

7 = Accretion after outcome (iii).

Figure 6: Eccentricity distribution as a function of time and particle size for Experiment #1. Inclinations are similar. Initial value, $e = 5 \times 10^{-4}$, is shown by +. Corresponding random velocities are shown on right hand scales in terms of 1 km escape velocity, $v_e \sim 20$ cm/sec.

Figure 7: Size distribution evolution for Experiment #2 with crater ejecta escape effectively suppressed but otherwise parameters and initial conditions are the same as for Experiment #1. Note similarity of growth.

Figure 8: Size distribution for Experiment #3 which was identical to Experiment #2, but with finer size resolution. Results are similar indicating that they are not limited by our coarse size bins.

Figure 9: Size distribution evolution for Experiment #4 which was identical to Experiment #1, except with 100 times as many initial bodies. Principal difference is contraction of the time scale.

Figure 10: Size distribution for a case (Experiment #5) using impact parameters appropriate for solid rock.

Figure 11: Collision outcome matrix for Experiment #5. See caption of Fig. 5 for code.

Figure 12: Velocity distribution for Experiment #5. Here, $v_e \sim 25$ cm/sec.

Figure 13: Size distribution for a case (Experiment #6), using impact parameters appropriate to weakly bonded regolith.

Figure 14: Collision outcome matrix for Experiment #6. See caption of Fig. 5 for code.

Figure 15: Velocity distribution for Experiment #6. Here $v_e \sim 10$ cm/sec.

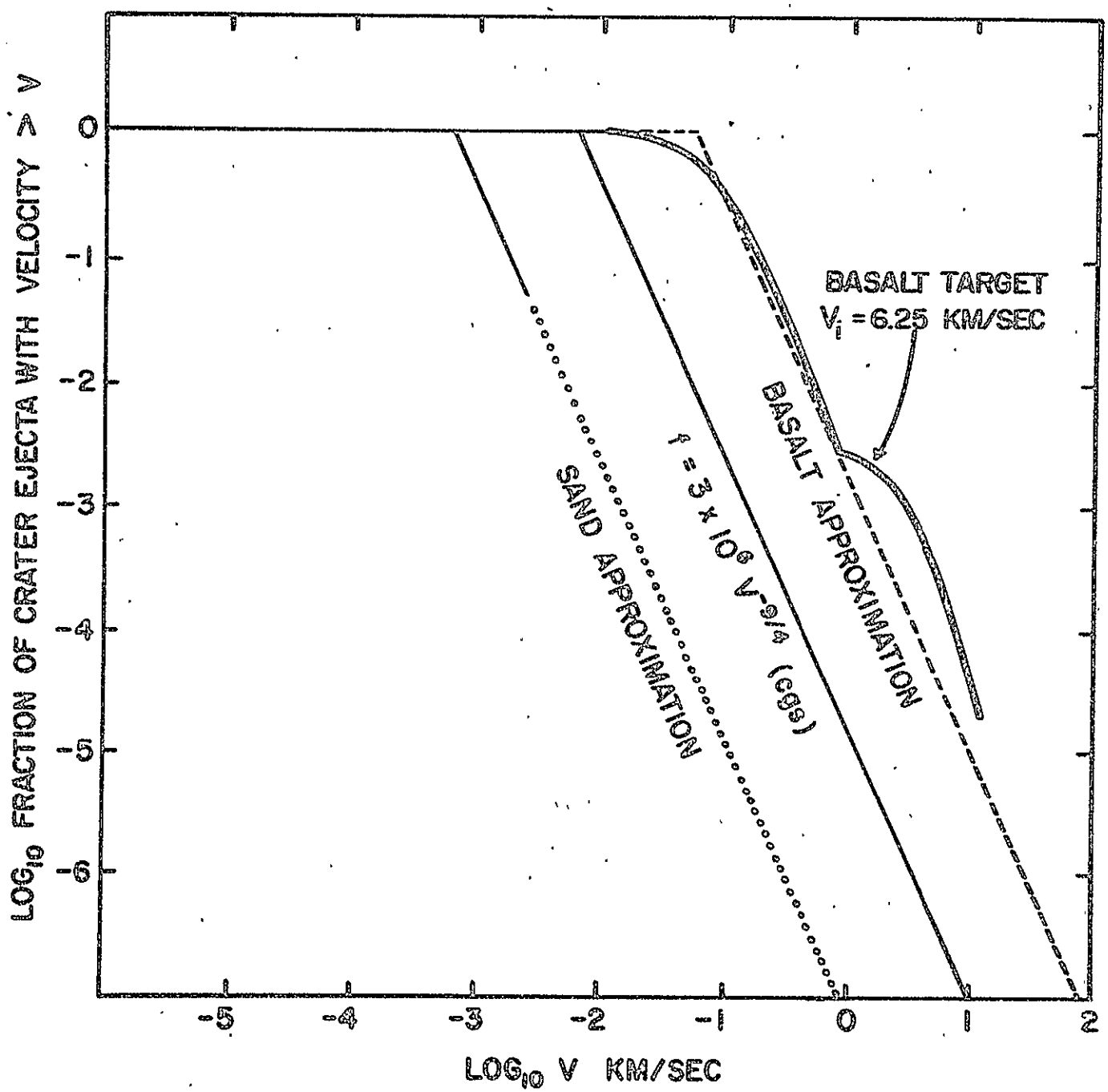
BASALT TARGET
V_i = 6.25 KM/SEC
BASALT APPROXIMATION
$f = 3 \times 10^6 V^{-9/4}$ (CGS)
SAND APPROXIMATION
LOG_{10} FRACTION OF CRATER EJECTA WITH VELOCITY > V
LOG_{10} V KM/SEC
0
-1
-2
-3
-4
-5
-6
-5
-4
-3
-2
-1
0
1
2

FIG. 1

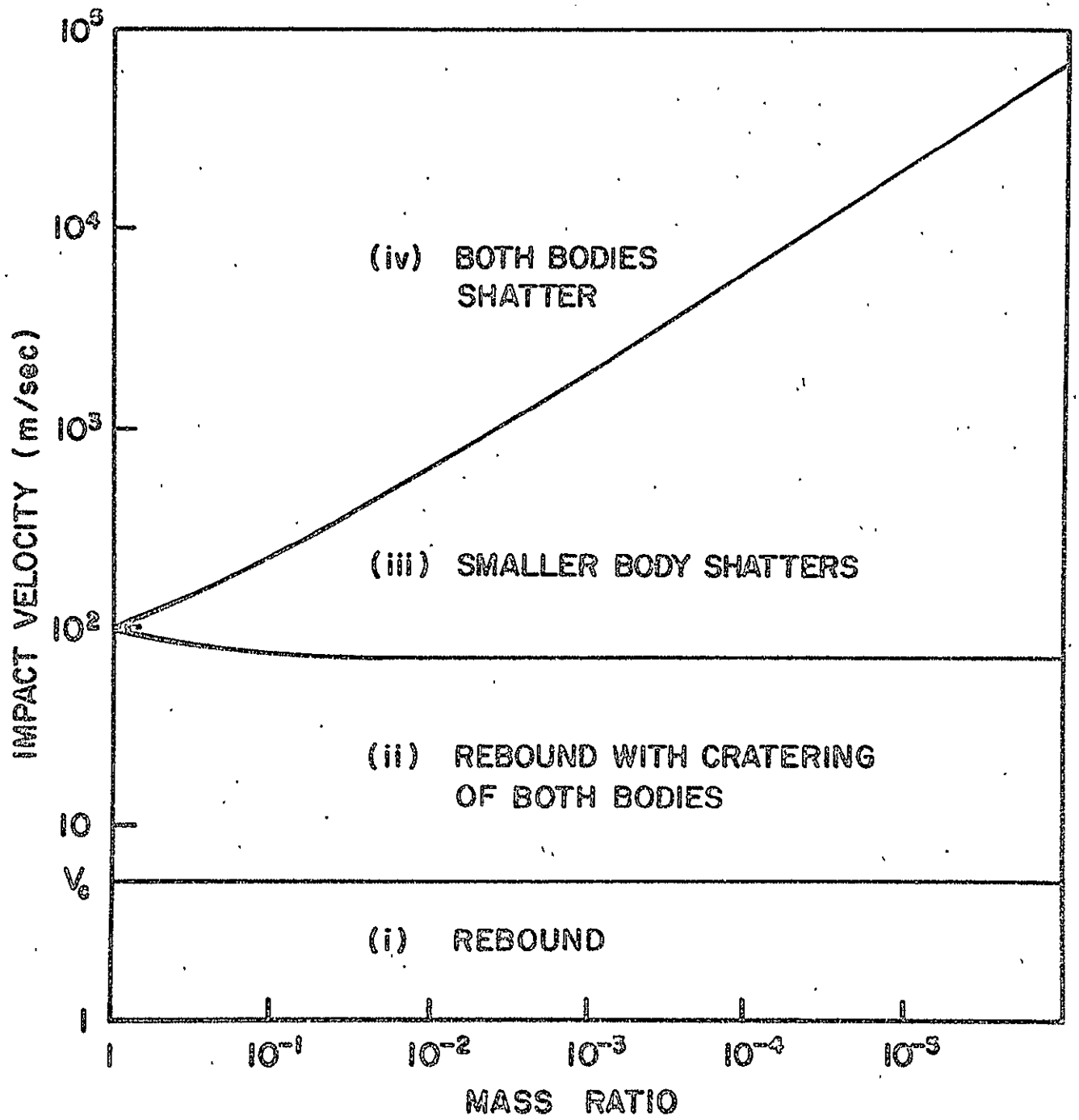
IMPACT VELOCITY (m/sec)
10^5
10^4
10^3
10^2
10
V_c
1
(iv) BOTH BODIES SHATTER
(iii) SMALLER BODY SHATTERS
(ii) REBOUND WITH CRATERING OF BOTH BODIES
(i) REBOUND
1
10^{-1}
10^{-2}
10^{-3}
10^{-4}
10^{-5}
MASS RATIO

FIG. 2

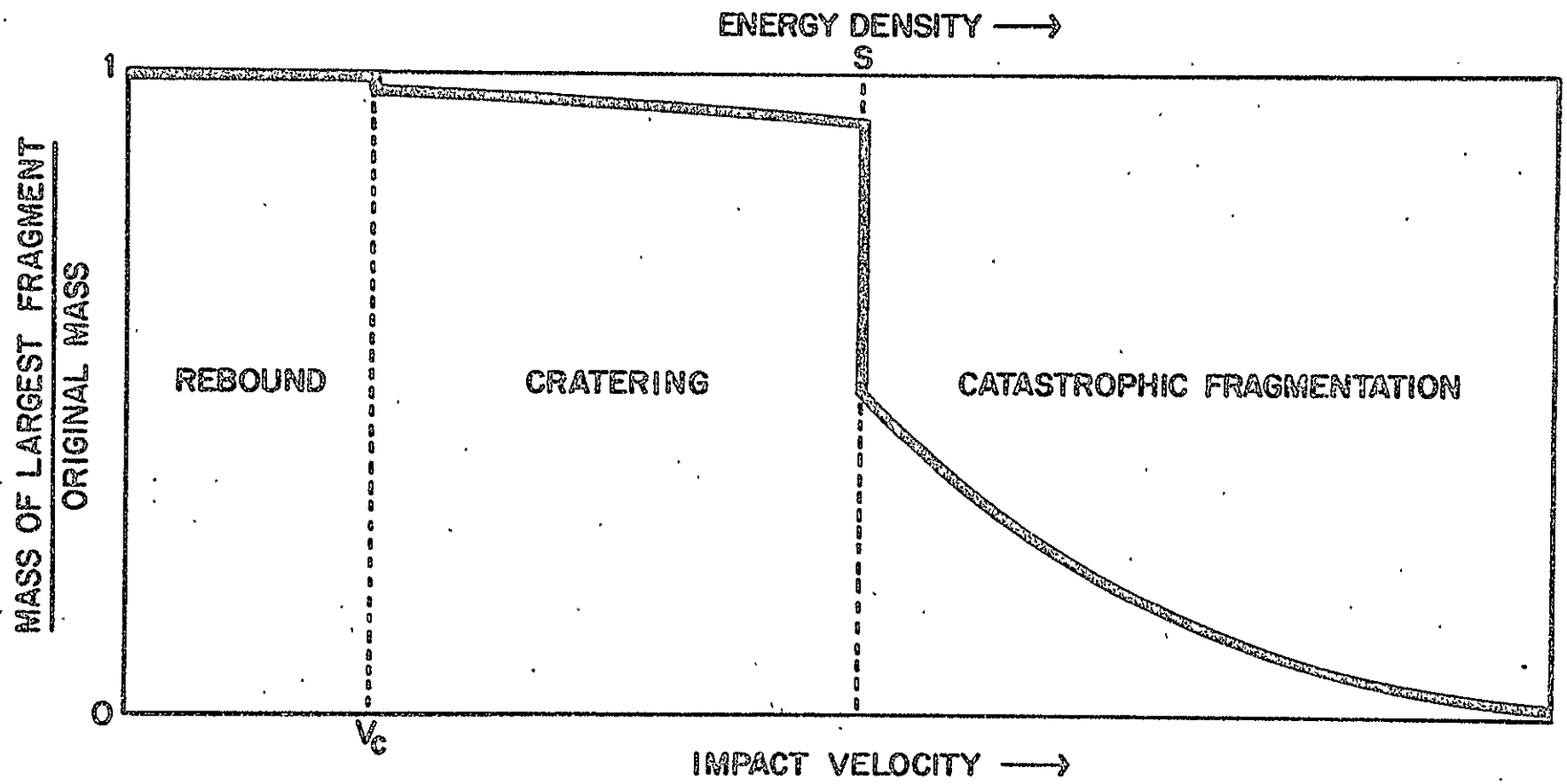
ENERGY DENSITY ⟶
S
1
0
MASS OF LARGEST FRAGMENT / ORIGINAL MASS
REBOUND
CRATERING
CATASTROPHIC FRAGMENTATION
V_c
IMPACT VELOCITY ⟶

FIGURE 3

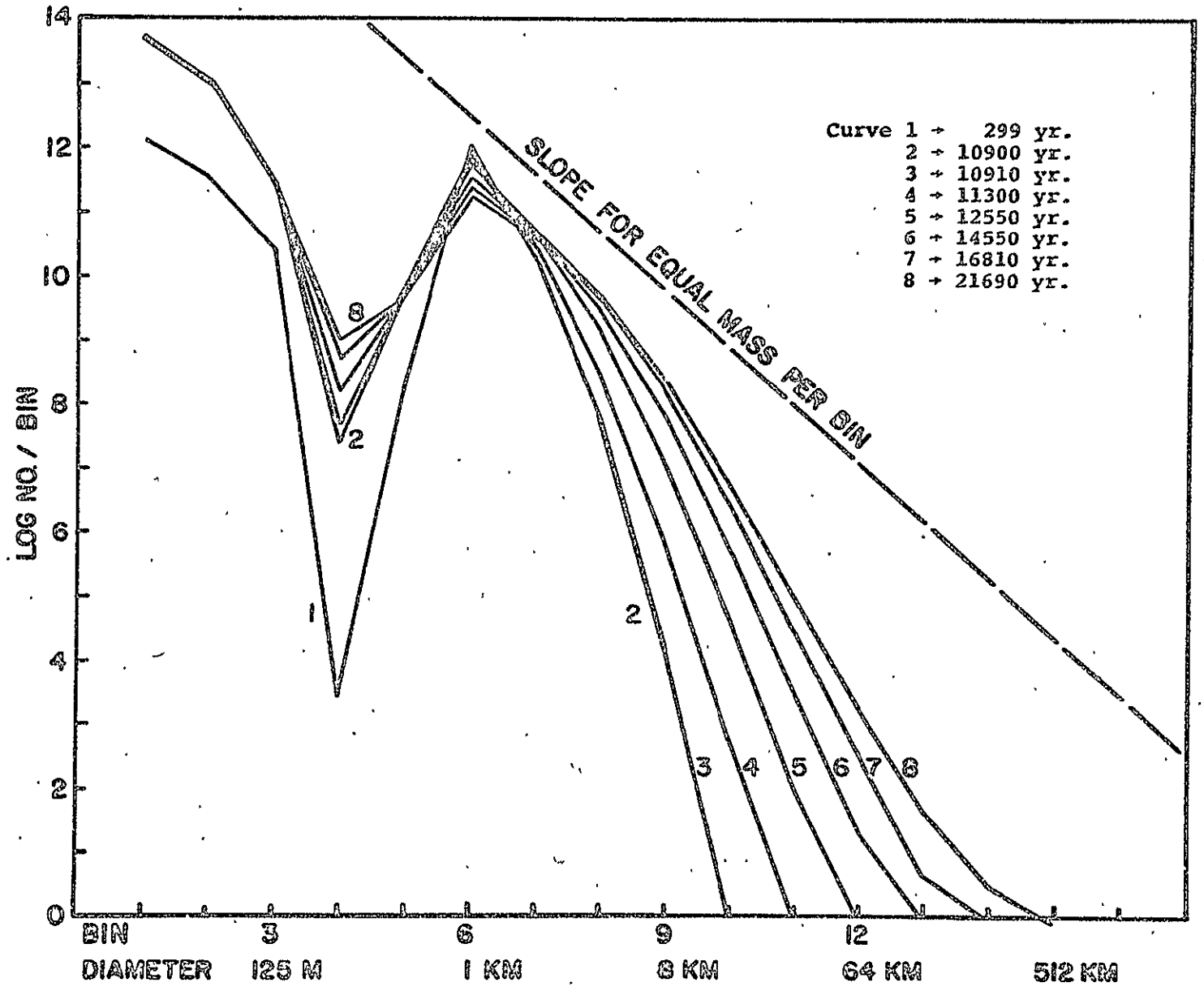
LOG NO. / BIN
14
12
10
8
6
4
2
0
BIN
3
6
9
12
DIAMETER
125 M
1 KM
8 KM
64 KM
512 KM
SLOPE FOR EQUAL MASS PER BIN
Curve 1 → 299 yr.
2 → 10900 yr.
3 → 10910 yr.
4 → 11300 yr.
5 → 12550 yr.
6 → 14550 yr.
7 → 16810 yr.
8 → 21690 yr.
1
2
3
4
5
6
7
8

FIGURE 4

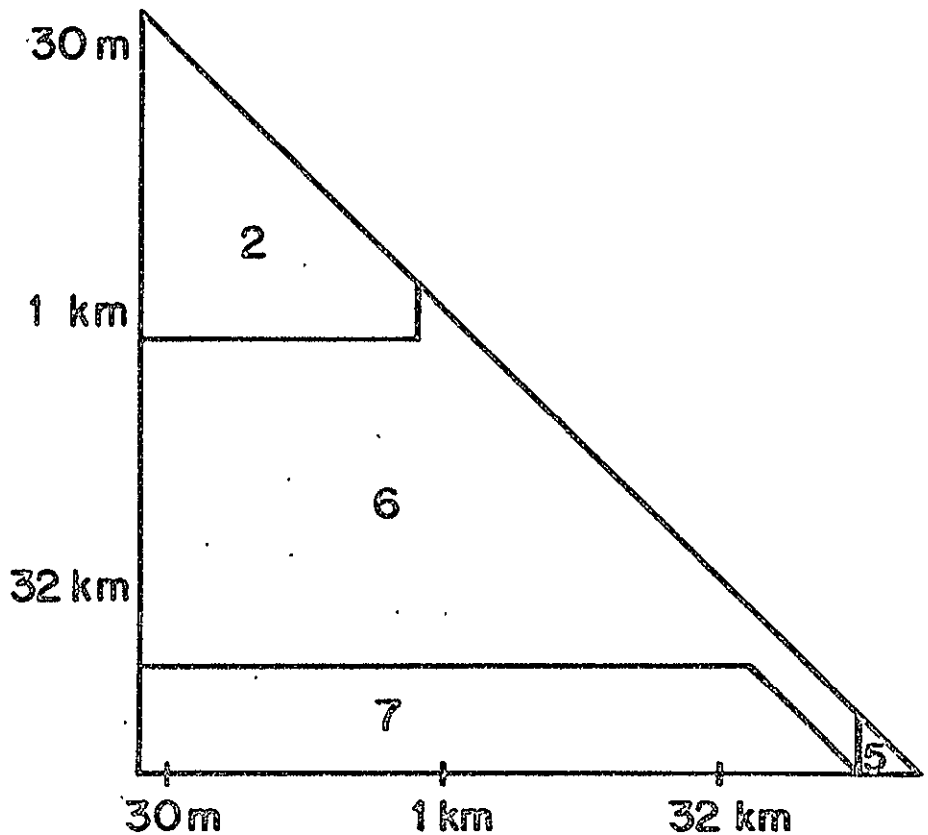

FIGURE 5

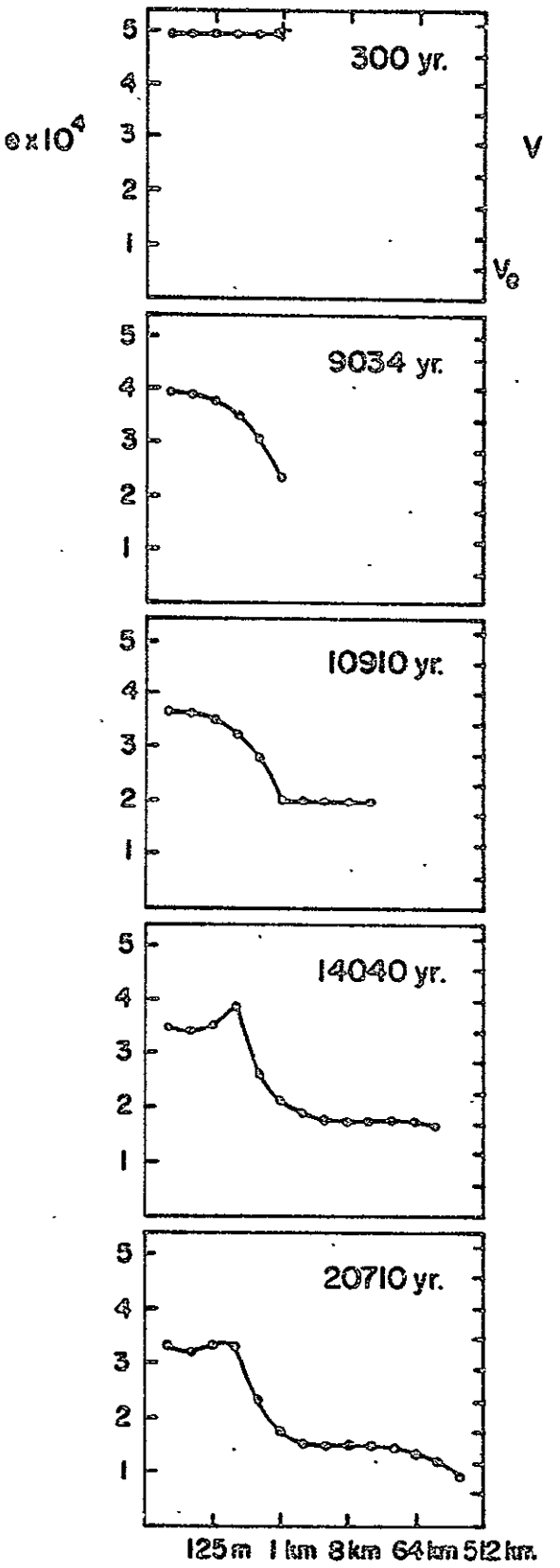
θ x 10^4
V
V_θ
300 yr.
9034 yr.
10910 yr.
14040 yr.
20710 yr.
125 m
1 km
8 km
64 km
512 km

FIGURE 6

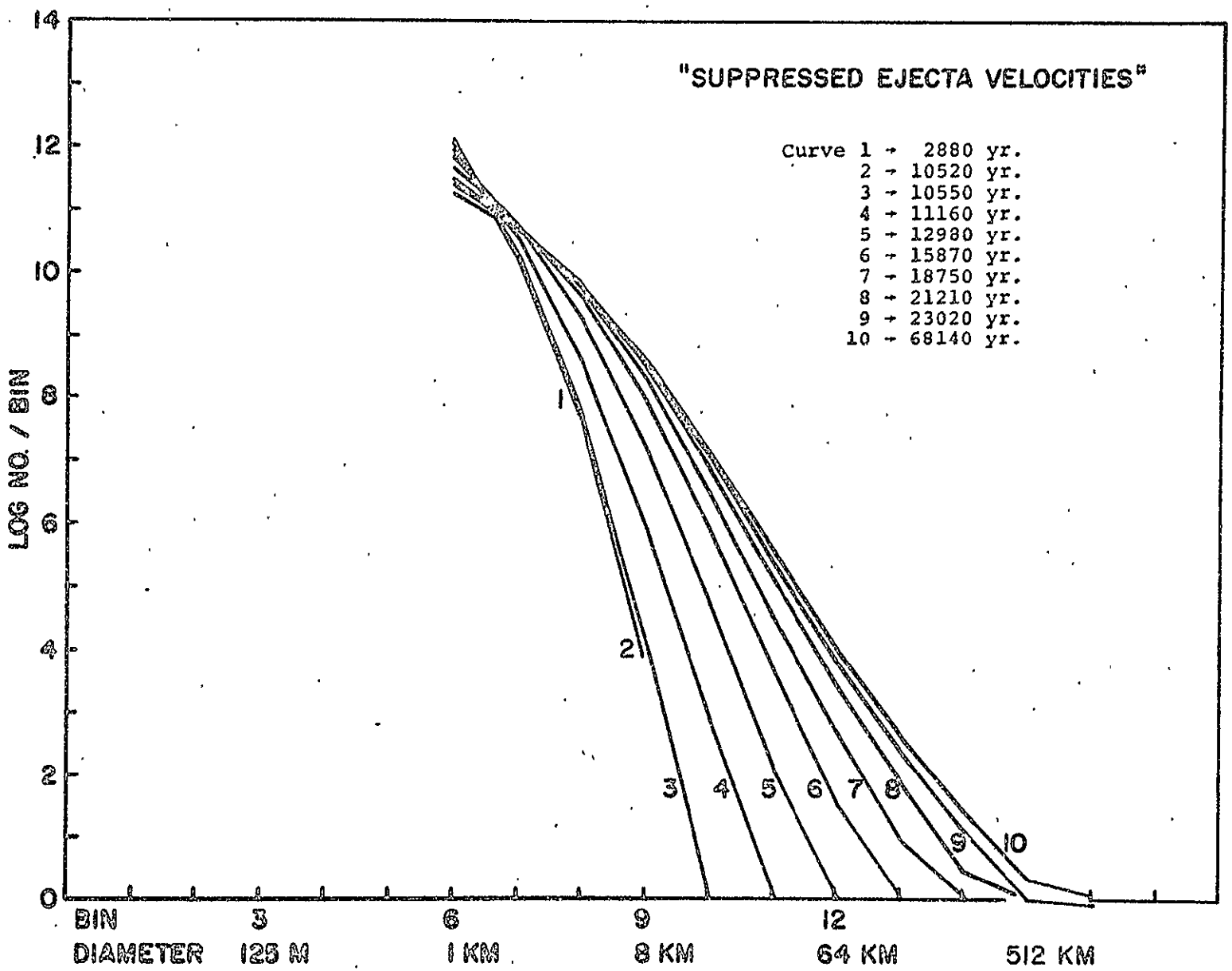
"SUPPRESSED EJECTA VELOCITIES"
Curve 1 → 2880 yr.
2 → 10520 yr.
3 → 10550 yr.
4 → 11160 yr.
5 → 12980 yr.
6 → 15870 yr.
7 → 18750 yr.
8 → 21210 yr.
9 → 23020 yr.
10 → 68140 yr.
LOG NO. / BIN
0
2
4
6
8
10
12
14
1
2
3
4
5
6
7
8
9
10
BIN
3
6
9
12
DIAMETER
125 M
1 KM
8 KM
64 KM
512 KM

FIGURE 7

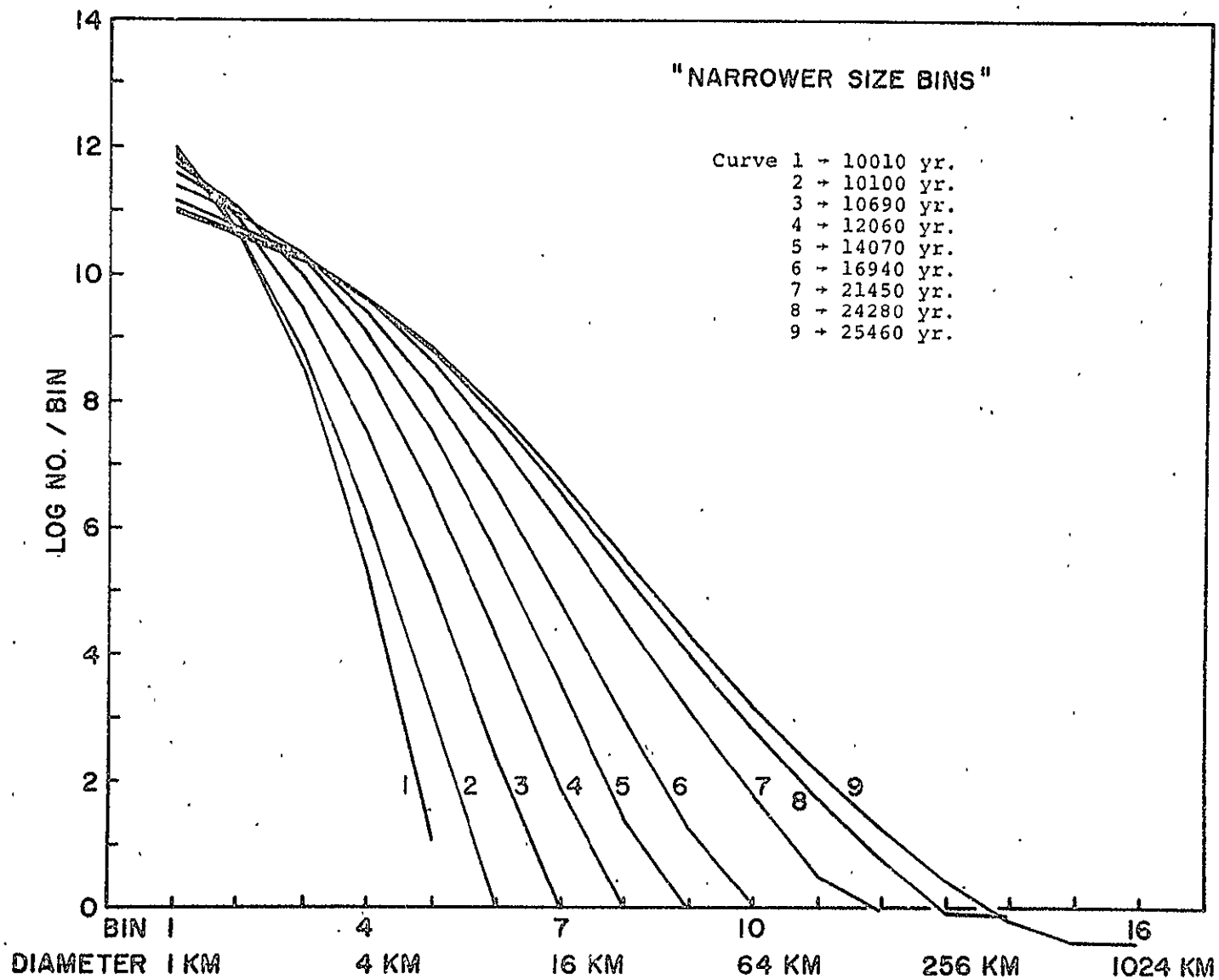
"NARROWER SIZE BINS"
Curve 1 → 10010 yr.
2 → 10100 yr.
3 → 10690 yr.
4 → 12060 yr.
5 → 14070 yr.
6 → 16940 yr.
7 → 21450 yr.
8 → 24280 yr.
9 → 25460 yr.
LOG NO. / BIN
0
2
4
6
8
10
12
14
1
2
3
4
5
6
7
8
9
BIN 1
4
7
10
16
DIAMETER 1 KM
4 KM
16 KM
64 KM
256 KM
1024 KM

FIGURE 8

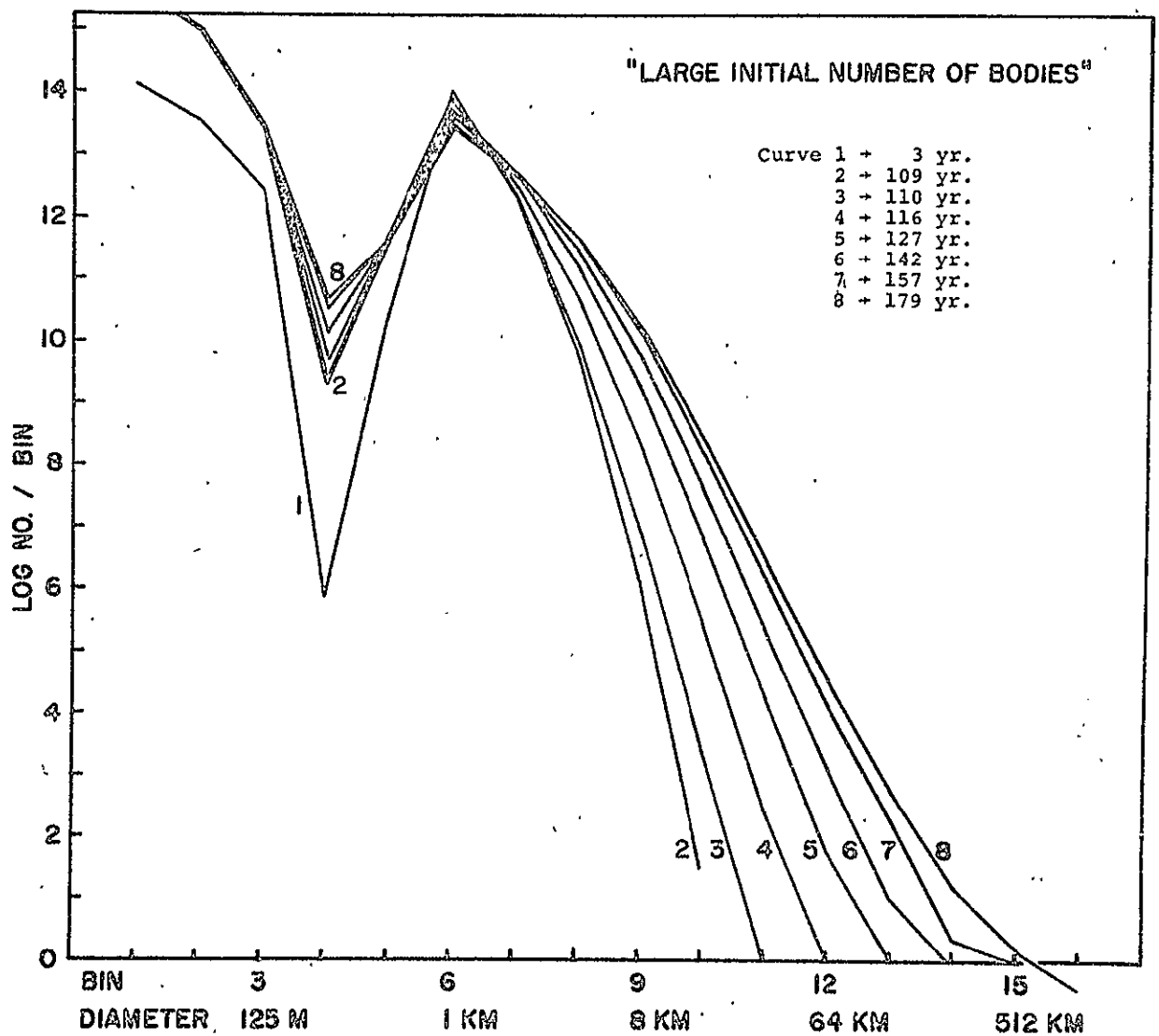
"LARGE INITIAL NUMBER OF BODIES"
Curve 1 → 3 yr.
2 → 109 yr.
3 → 110 yr.
4 → 116 yr.
5 → 127 yr.
6 → 142 yr.
7 → 157 yr.
8 → 179 yr.
LOG NO. / BIN
0
2
4
6
8
10
12
14
BIN
3
6
9
12
15
DIAMETER, 125 M
1 KM
8 KM
64 KM
512 KM
1
2
8
2
3
4
5
6
7
8

FIGURE 9

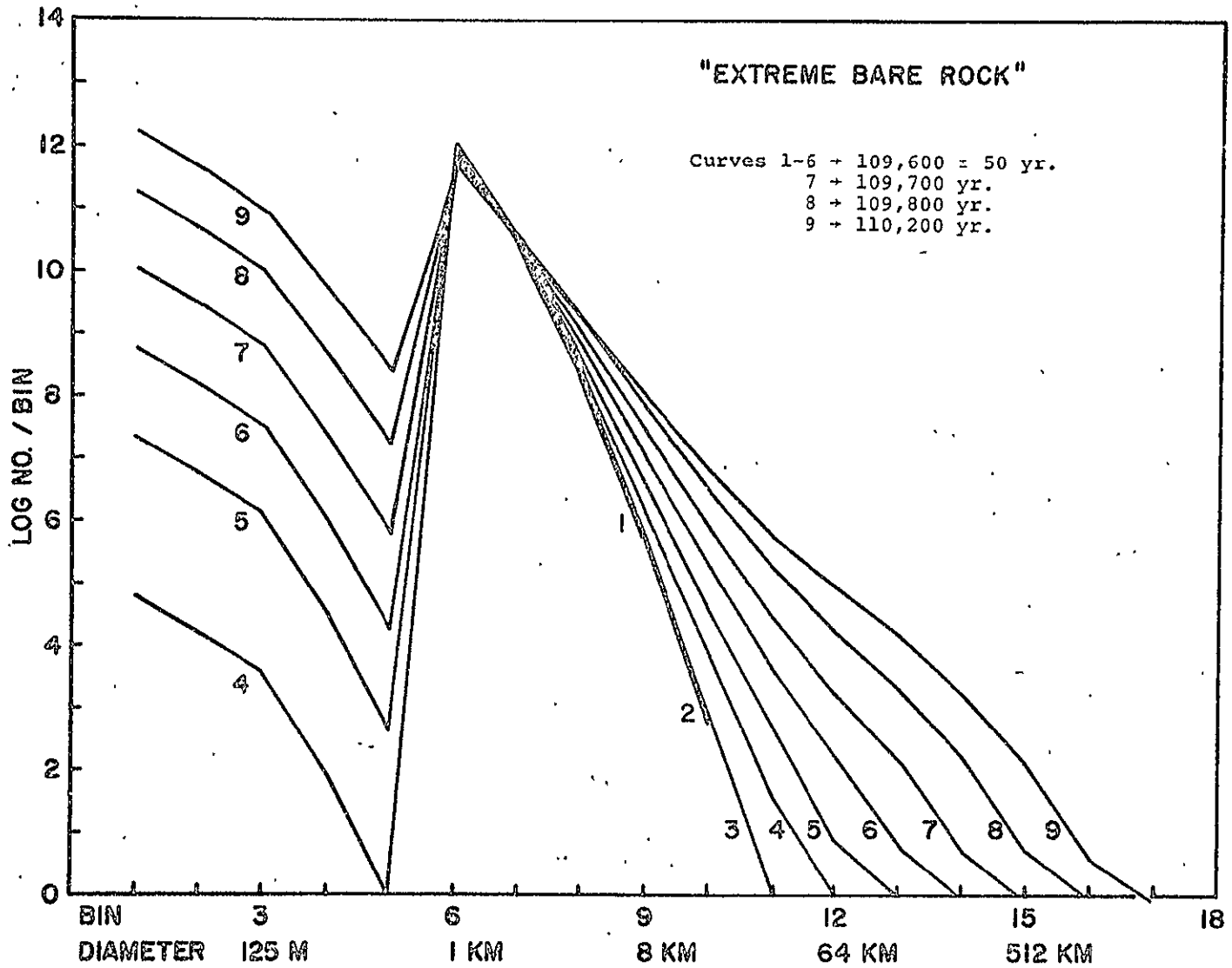
"EXTREME BARE ROCK"
Curves 1-6 → 109,600 ± 50 yr.
7 → 109,700 yr.
8 → 109,800 yr.
9 → 110,200 yr.
LOG NO. / BIN
0
2
4
6
8
10
12
14
BIN
DIAMETER
3
125 M
6
1 KM
9
8 KM
12
64 KM
15
512 KM
18
1
2
3
4
5
6
7
8
9

FIGURE 10

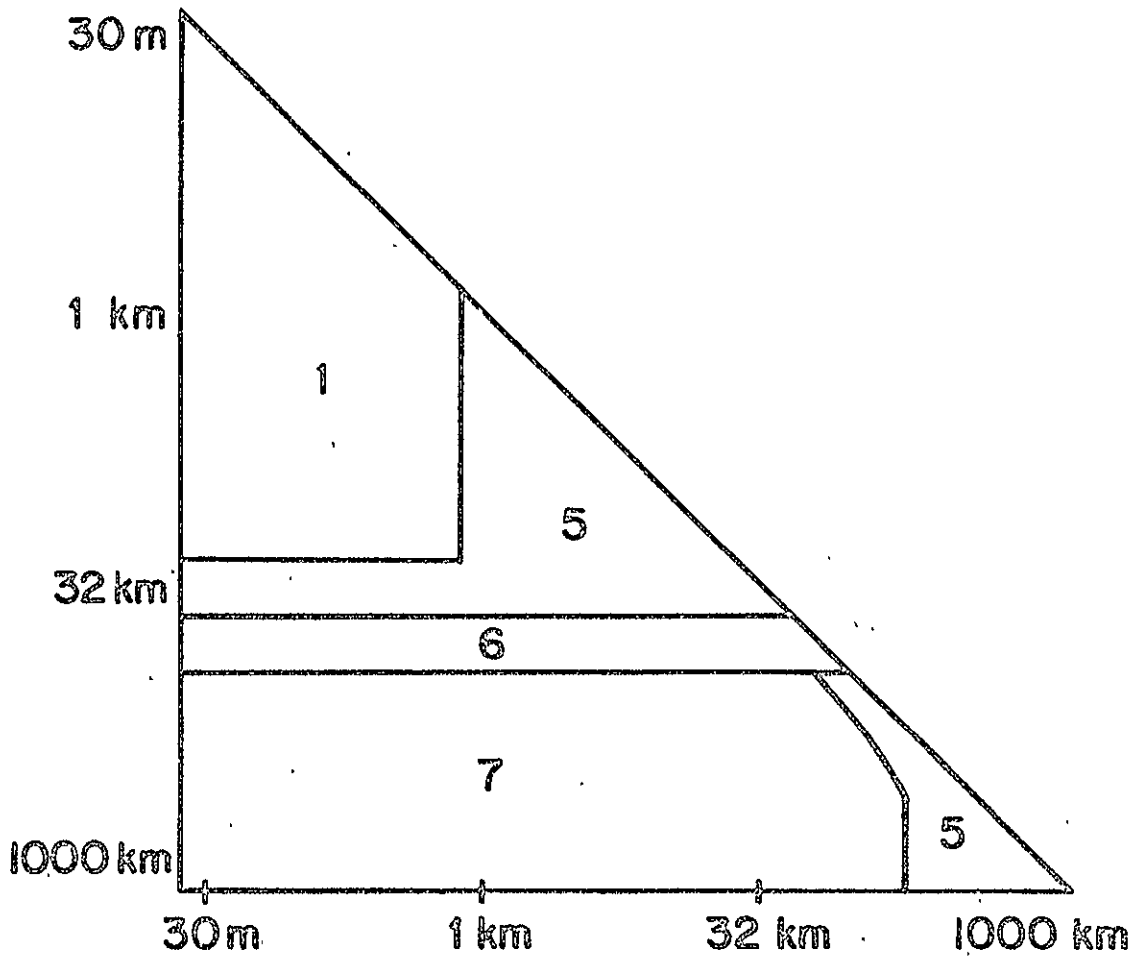

FIGURE 11

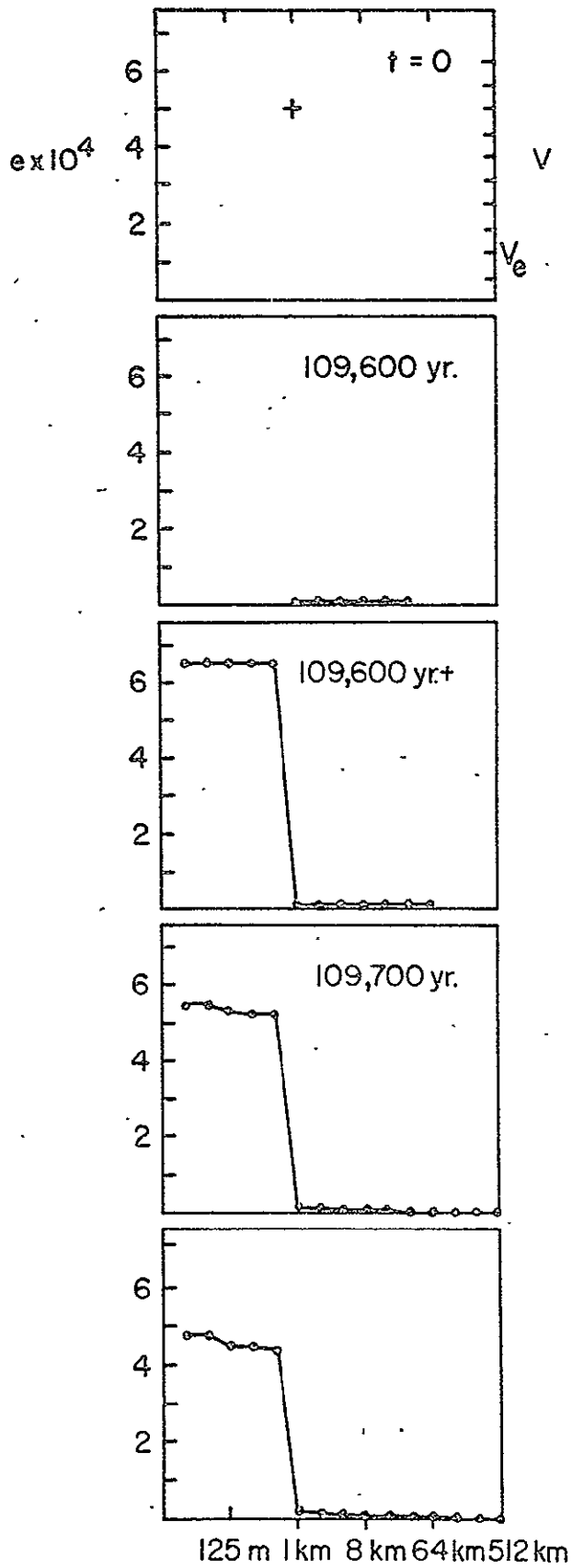
t = 0
109,600 yr.
109,600 yr.+
109,700 yr.
e x 10^4
V
V_e
6
4
2
125 m
1 km
8 km
64 km
512 km

FIGURE 12

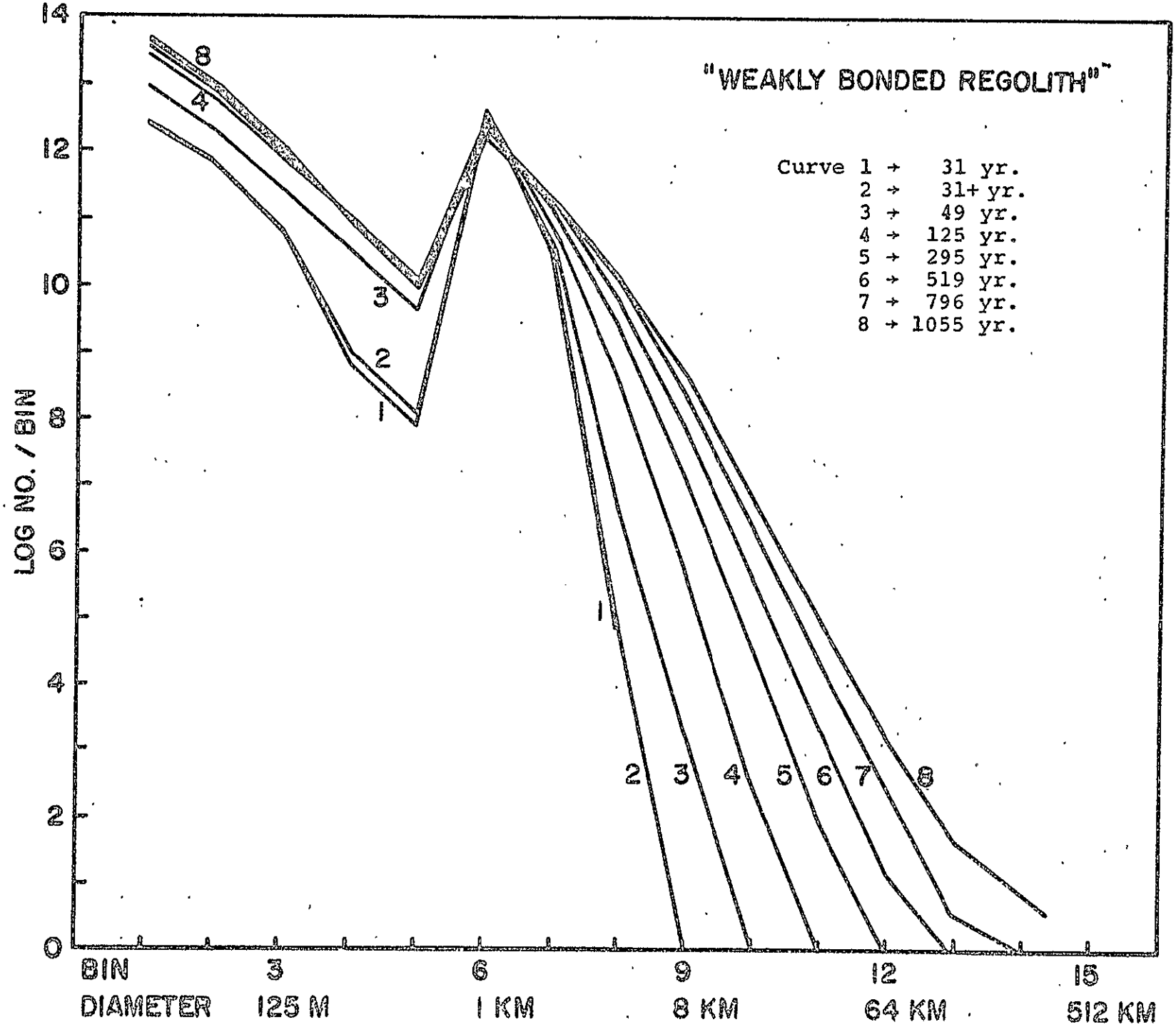
"WEAKLY BONDED REGOLITH"
Curve 1 → 31 yr.
2 → 31+ yr.
3 → 49 yr.
4 → 125 yr.
5 → 295 yr.
6 → 519 yr.
7 → 796 yr.
8 → 1055 yr.
LOG NO. / BIN
0
2
4
6
8
10
12
14
BIN
DIAMETER
3
125 M
6
1 KM
9
8 KM
12
64 KM
15
512 KM
1
2
3
4
5
6
7
8

FIGURE 13

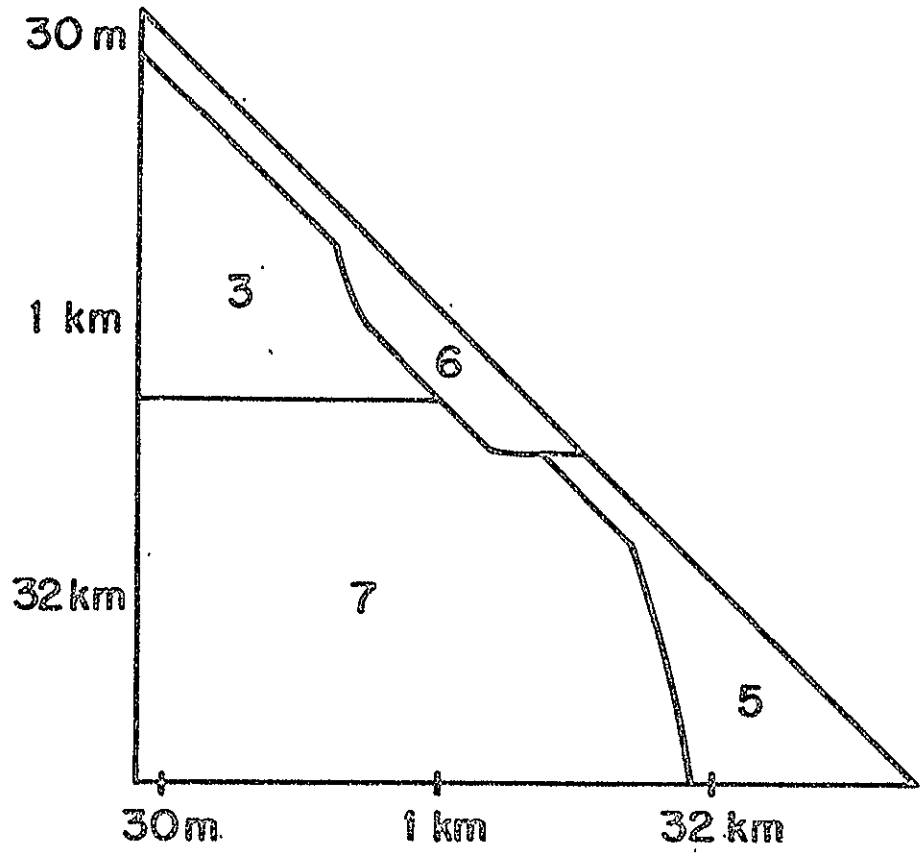

FIGURE 14

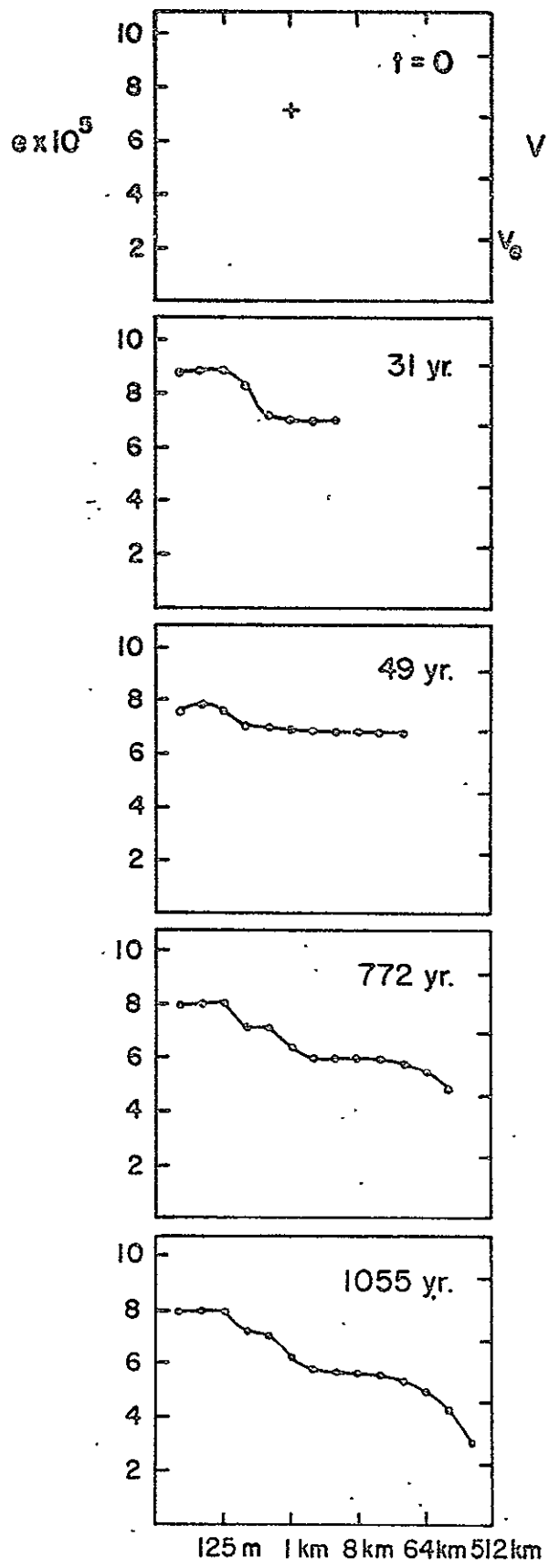
e x 10^5
10
8
6
4
2
t = 0
V
V_e
31 yr.
49 yr.
772 yr.
1055 yr.
125 m
1 km
8 km
64 km
512 km

FIGURE 15